Check for updates

Received: 13 May 2026 | Revised: 19 August 2026 | Accepted: 7 September 2026

DOI: 10.1111/bph.70698

RESEARCH ARTICLE

Crossing subfamily borders: Mechanosensitive TREK-1 and alkaline-activated TASK-4 form heterodimers with unique functional and pharmacological properties

Sven Schütte[1] | Florian Schick[1] | Emilia De Martino[1] | Hannah Schmitz[1] | Katharina E. S. Zander[1] | Franziska Holz[2] | Patrick Sauer[2] | Luise Mildeberger[2] | Moritz Linder[3] | Axel Loewe[3] | Aytug K. Kiper[1,4] | Silke Kauferstein[2,5] | Martin K.-H. Schäfer[6] | Susanne Rinné[1] | Niels Decher[1]

[1]Institute of Physiology and Pathophysiology, Vegetative Physiology, University of Marburg, Marburg, Germany

[2]Department of Legal Medicine, Goethe University, University Hospital Frankfurt, Frankfurt am Main, Germany

[3]Institute of Biomedical Engineering, Karlsruhe Institute of Technology (KIT), Karlsruhe, Germany

[4]Institute of Physiology, University Medicine Greifswald, Greifswald, Germany

[5]DZHK (German Centre for Cardiovascular Research), Partner Site Rhein-Main, Frankfurt/Main, Germany

[6]Institute of Anatomy and Cell Biology, Medical Cell Biology, University of Marburg, Marburg, Germany

Correspondence
Niels Decher, Institute of Physiology and Pathophysiology, Vegetative Physiology, University of Marburg, 35037 Marburg, Germany.
Email: decher@staff.uni-marburg.de

Funding information
Deutsche Forschungsgemeinschaft, Grant/Award Number: DE1482/9-1; Studienstiftung des deutschen Volkes;

Background and Purpose: The tandem of two-pore-domain potassium (K_{2P}) channels TREK-1 and TASK-4 are expressed in the heart and pancreatic beta-cells. As TREK-1 and TASK-4 belong to distinct subfamilies with different functional hallmarks, heteromerization of these two channels was highly unexpected. However, due to their shared expression in these tissues and their involvement in congenital cardiac arrhythmias, the aim of this study was to probe for a possible formation of TREK-1/TASK-4 heterodimers.

Experimental Approach: Two-electrode voltage-clamp and inside-out macropatch clamp recordings, together with immunohistochemistry and chemiluminescence-based ELISA assays, were utilized to describe heteromerization of TREK-1 and TASK-4 channels and elucidate the characteristics of this heteromeric channel complex.

Key Results: Here, we show that the mechanosensitive TREK-1 forms heteromeric channel complexes with the alkaline-activated TASK-4. The resulting heterodimers of these only remotely related channels have an enhanced temperature sensitivity, an altered pH dependence and regulation by extracellular sodium. Unlike TREK-1, heteromeric TREK-1/TASK-4 channels are not inhibited via G_s-coupled receptor activation, as the heterodimeric channels are not PKA sensitive. Strikingly, these novel heterodimeric channel complexes are characterized by a unique pharmacology.

Conclusions and Implications: The newly described heterodimerization across different K_{2P} channel families is of major relevance for drugs targeting TASK-4 or TREK-1.

Abbreviations: BSA, bovine serum albumin; FFPE, PFA-fixed paraffin-embedded; HA-Ex, extracellular haemagglutinin; IBMX, 3-isobutyl-1-methylxanthine; iVF, idiopathic ventricular fibrillation; K_{2P}, two-pore-domain potassium channel; LQTS, long-QT syndrome; NMDG, N-methyl-D-glucamine; PCCD, progressive cardiac conduction disorder; POPDC, Popeye domain containing; Q_{10}, temperature coefficient; RLUs, relative light units; RVOT-VT, right ventricular outflow tract ventricular tachycardia; SSRIs, serotonin-specific reuptake inhibitors; TALK, TWIK-related alkaline-pH-activated K^+ channel; TASK, TWIK-related acid-sensitive K^+ channel; TPA-Cl, tetrapentylammonium chloride; TREK, TWIK-related K^+ channel; TRESK, TWIK-related spinal cord K^+ channel.

Sven Schütte and Florian Schick are joint first authors.

Susanne Rinné and Niels Decher are joint last authors.

This is an open access article under the terms of the Creative Commons Attribution License, which permits use, distribution and reproduction in any medium, provided the original work is properly cited.

© 2026 The Author(s). *British Journal of Pharmacology* published by John Wiley & Sons Ltd on behalf of British Pharmacological Society.

Medizinstiftung der Philipps-Universität Marburg

Their functional co-expression in different tissues raises the possibility of developing drugs against cardiac arrhythmias and Type 2 diabetes by specifically targeting these unique heterodimeric channel complexes.

KEYWORDS
molecular pharmacology, signal transduction, the tandem of two-pore-domain potassium (K_{2P}) channels

1 | INTRODUCTION

The **two-pore-domain potassium (K_{2P}) channel family** consists of 15 members that are divided into six subfamilies based on their structural and functional properties (Feliciangeli et al., 2015). K_{2P} channel subunits assemble as dimers to form background channels essential for maintaining the resting membrane potential. Their polymodal regulation by a variety of chemical or physical stimuli is responsible for the adaptation of the leak potassium currents to cellular needs. Heteromerization of potassium channels has been well described to increase the diversity of potassium currents. For K_{2P} channels, it was anticipated that heteromerization primarily occurred within a subfamily; however, recently, heterodimerization between K_{2P} subunits from different subfamilies has also been reported (Khoubza et al., 2021). K_{2P} channels are of major physiological relevance and play a role in many diseases, such as epilepsy, cardiac arrhythmias and pulmonary hypertension. There is growing evidence that K_{2P} channel heterodimers contribute to those (patho)physiological mechanisms (Khoubza et al., 2021). Because heteromerization significantly influences the pharmacology of K_{2P} channels (Khoubza et al., 2021; Rinné et al., 2024), these heteromers are emerging as promising drug targets against various diseases.

TREK-1 (*KCNK2*) currents are sensitive to mechanical stimulation (Patel et al., 1998) and changes in temperature (Maingret et al., 2000), which are hallmarks of the TREK subfamily. TREK-1 is expressed in a wide variety of tissues, including the central and peripheral nervous system, skeletal and smooth muscle, lung, heart, kidney, pancreas, stomach and small intestine (Fink et al., 1996; Medhurst et al., 2001; Schmidt et al., 2015; Schmidt, Wiedmann, Kallenberger, et al., 2017; Talley et al., 2001; Tertyshnikova et al., 2005; Viatchenko-Karpinski et al., 2018). The channel is polymodally regulated, and besides its mechanical and temperature sensitivity, TREK-1 is activated by lipids, polyunsaturated fatty acids (Danthi et al., 2003; Riel et al., 2022) or intracellular acidification (Maingret et al., 1999). In contrast, TREK-1 currents are reduced by **PKA**- and **PKC**-dependent phosphorylation (Murbartian et al., 2005) and by extracellular acidification (Cohen et al., 2008). TREK-1 is also modulated by interacting proteins, such as the proteins of the Popeye domain containing (POPDC) family (Decher, Kiper, & Rinné, 2017; Froese et al., 2012; Sandoz et al., 2006; Sandoz et al., 2008; Schindler et al., 2016; Vissing et al., 2019). Another hallmark of TREK-1 is its sensitivity to **serotonin-specific reuptake** inhibitors (SSRIs) such as **fluoxetine** or **norfluoxetine**, which is thought to play a role in the antidepressant action of SSRIs (Kennard et al., 2005). TREK-1 forms heterodimeric channels with the other members of the stretch-activated K_{2P} channel family (Blin et al., 2016; Lengyel et al., 2016). However, heterodimer formation was also described with **TWIK-1** (Hwang et al., 2014) and **TRESK** channels (Royal et al., 2019). Recent studies on the (patho) physiological role of TREK-1 in the heart found that the channel is relevant in atrial fibrillation and in inherited forms of ventricular tachyarrhythmias (right ventricular outflow tract ventricular tachycardias [RVOT-VTs]) (Decher, Ortiz-Bonnin, et al., 2017; Schmidt, Wiedmann, Kallenberger, et al., 2017). The role of TREK-1 in the heart, and particularly in the cardiac conduction system, is further supported by mutations in POPDC1 and POPDC2 (Rinné et al., 2020; Schindler et al., 2016) or their respective knock-down or knock-out (Froese et al., 2012; Kirchmaier et al., 2012; Simrick et al., 2013), as POPDC proteins modulate TREK-1. Here, similar to the TREK-1 knock-out

What is already known?

- K_{2P} channels typically form dimers within subfamilies to generate background potassium currents.
- TREK-1/TASK-4 are co-expressed in cardiac and pancreatic beta-cells and linked to cardiac arrhythmias and diabetes.

What does this study add?

- TREK-1 and TASK-4 form unexpected inter-subfamily heteromers with biophysical properties distinct from their respective homodimers.
- These heteromers exhibit a unique pharmacological profile and cause a loss of G_s-coupled receptor signalling.

What is the clinical significance?

- TREK-1/TASK-4 heteromers provide a novel target for specific antiarrhythmic and antidiabetic drug development.
- Our observations are essential to predict heteromerization-dependent *in vivo* drug potency and avoid off-target effects.

14765381, 0, Downloaded from https://bpspubs.onlinelibrary.wiley.com/doi/10.1111/bph.70698 by Karlsruher Institut Fur Technologie, Wiley Online Library on [16/11/2026]. See the Terms and Conditions (https://onlinelibrary.wiley.com/terms-and-conditions) on Wiley Online Library for rules of use; OA articles are governed by the applicable Creative Commons License

mice (Unudurthi et al., 2016), an atrioventricular (AV) block and/or a sick sinus syndrome was observed. In addition, TREK-1 may play a role in the control of insulin secretion (Hivelin et al., 2016).

TASK-4 (*KCNK17*; also known as TALK-2), is expressed in a variety of tissues, with the highest levels in the pancreas, liver, placenta, small intestine and aorta but also the heart (Decher et al., 2001; Girard et al., 2001). In the latter, it is found with a more pronounced expression in the conduction system and atrial tissue (Decher et al., 2001; Friedrich et al., 2014). The common feature of this channel subfamily, which includes TALK-1 and TASK-2, is the activation by extracellular alkalization. In addition, TASK-4 is activated by lipids including oleoyl-CoA and PIP_2 (Riel et al., 2022), as well as by reactive oxygen species (ROS) and **nitric oxide** (Duprat et al., 2005). Many antiarrhythmic drugs, including **amiodarone**, **sotalol**, **verapamil**, **quinidine**, **propranolol** or **metoprolol** activate or block TASK-4 channels, albeit at only very high drug concentrations (Staudacher et al., 2018). TASK-4 forms heterodimeric channels within its own subfamily members (Khoubza et al., 2021), and heterodimerization with TASK-1 has also been reported (Suzuki et al., 2017). Like TREK-1, TASK-4 is of cardiac (patho)physiological relevance, and gain-of-function mutations in *KCNK17* have been linked to progressive cardiac conduction disorder (PCCD) accompanied by idiopathic ventricular fibrillation (iVF) (Friedrich et al., 2014). In addition, a gain-of-function polymorphism in TASK-4 protects against long-QT syndrome (LQTS) (Chai et al., 2018). On the other hand, reduced expression of TASK-4 was found in patients with chronic atrial fibrillation or with left ventricular dysfunction (Schmidt et al., 2015; Schmidt, Wiedmann, Zhou, et al., 2017). Besides its role in the heart, TASK-4 is one of the three most abundant potassium channel transcripts in human beta-cells (Blodgett et al., 2015). Several genetic polymorphisms have been described that are highly likely to increase the expression of TASK-4 or lead to a gain-of-function (Chai et al., 2018; Dobson et al., 2026; Varshney, Scott et al., 2017), which may confer diabetes risk through multiple pathophysiological mechanisms affecting beta cell calcium handling and insulin secretion (Dobson et al., 2026).

Here, we describe the unexpected heterodimerization of TASK-4, a member of the alkaline-activated K_{2P} channel subfamily, with TREK-1, a member of the mechanosensitive subfamily of K_{2P} channels. Unlike TREK-1, heteromeric TREK-1/TASK-4 channels are not inhibited by **G_s-coupled receptor** activation due to a lack of PKA sensitivity, and they show increased temperature sensitivity, as well as an altered extracellular pH dependence. Notably, the heteromeric channels exhibit a distinct pharmacology, which is relevant for drugs targeting TASK-4 or TREK-1. Accounting for these properties is essential to correctly identify the underlying currents in normal tissues and to target them pharmacologically, thereby facilitating the development of more specific drugs with fewer side effects.

2 | METHODS

2.1 | Cloning and site-directed mutagenesis

Human (h)TREK-1b (AF004711), hTASK-4 (AF358910.1), hβ_1 adrenoceptor (NM_000684.3), hGLP-1 receptor (NM_002062.5) and hPOPDC1 (NM_147147.4) cDNAs were subcloned into the pFAW vector or the oocyte expression vector pSGEM. Subsequent linearization was performed using the NheI or MluI restriction enzyme. The QuikChange Site-Directed Mutagenesis Kit (Agilent) was used to introduce mutations into the constructs according to the manufacturer's instructions. This was followed by Sanger sequencing (Seqlab) to confirm correct amino acid exchange.

2.2 | Isolation of *Xenopus laevis* oocytes, cRNA synthesis and injection

All animal care and experimental procedures for the study using *Xenopus* frogs was approved by the Ethics Committee of the Regierungspräsidium Giessen (Protocol Code V54-19c 20 15 h 02 MR 20/28 Nr. V 16/2022). Animal studies are reported in compliance with the ARRIVE guidelines (Percie du Sert et al., 2020) and with the recommendations made by the *British Journal of Pharmacology* (Lilley et al., 2020).

Xenopus laevis frogs were obtained from Xenopus-I Inc. (Dexter, MI, USA) and kept under controlled environmental conditions (18°C–22°C, pH 7.4, 12h light/dark cycle, staple fish food pallets twice a week).

Oocytes were surgically retrieved from female *Xenopus laevis* frogs (age 4–13 years) anaesthetized with 0.15% tricaine. The extracted ovarian lobes were incubated in OR2 solution containing (in mM) 82.5 NaCl, 2 KCl, 1 $MgCl_2$ and 5 HEPES (pH 7.5 with NaOH/HCl), supplemented with collagenase (1.5 $mg \cdot ml^{-1}$) (Nordmark) to remove residual connective tissue. Subsequently, oocytes were stored in ND96 solution containing (in mM) 96 NaCl, 2 KCl, 1.8 $CaCl_2$, 1 $MgCl_2$ and 5 HEPES (pH 7.5 with NaOH/HCl), supplemented with Na-pyruvate (275 $mg \cdot L^{-1}$), theophylline (90 $mg \cdot L^{-1}$) and gentamicin (50 $mg \cdot L^{-1}$) (Sigma) (AB solution) at 18°C. For experiments with hPOPDC1 and GPCRs, injected *Xenopus* oocytes were kept in a solution without theophylline.

For *in vitro* transcription, the HiScribe T7 ARCA mRNA Kit (New England Biolabs) or the mMessage mMachine SP6 mRNA Kit (Invitrogen) was used following the manufacturer's instructions. Quantity and quality of cRNAs were assessed by agarose gel electrophoresis and spectrophotometry (NanoDrop 2000c, Thermo Fisher Scientific). Stage V and VI oocytes (Weber, 1999) were injected with 25–50 nl of cRNA each using borosilicate glass capillaries (3-000-203-G/X; Drummond) and a Nanoject II microinjector (Süd-Laborbedarf GmbH). Subsequently, the oocytes were used for measurements 2–3 days after injection.

2.3 | Two-electrode voltage-clamp recordings

Unless otherwise specified, all electrophysiological recordings were carried out at room temperature (20°C–22°C) with an Axon Axoclamp 900A Microelectrode Amplifier (Molecular Devices) and a Digidata 1440 Series analog/digital converter (Axon Instruments) or with a TurboTEC 10CD (npi) amplifier and a Digidata 1200 Series (Axon

14765381, 0, Downloaded from https://bpspubs.onlinelibrary.wiley.com/doi/10.1111/bph.70698 by Karlsruher Institut Fur Technologie, Wiley Online Library on [16/11/2026]. See the Terms and Conditions (https://onlinelibrary.wiley.com/terms-and-conditions) on Wiley Online Library for rules of use; OA articles are governed by the applicable Creative Commons License

Instruments). The micropipettes, made from borosilicate glass capillaries (GB 150TF-8P, Science Products), were pulled using a DMZ-Universal Puller (Zeitz) and had a resistance of 0.3–1.2 MΩ when filled with 3 M KCl solution. ND96 solutions with varying pH values were used for the recordings. Clampex 10 was used for data acquisition (Molecular Devices). Clampfit 10, Office Excel (Microsoft) and Origin 2016 (OriginLab Corp.) were used for data analysis.

Current amplitudes were analysed at +40 mV after applying a ramp protocol. From a holding potential of −80 mV, the voltage was ramped from −120 to +45 mV within 3.5 s. Pharmacological modulation was recorded with voltage steps from a holding potential of −80 mV. A first test pulse to 0 mV of 1 s duration was followed by a repolarizing step to −80 mV for 1 s and a subsequent test pulse to +40 mV for another 1 s. The inter-sweep time interval, for both the ramp and the voltage step protocol, was 10 s. pH dependence was measured with a ramp protocol starting from a holding potential of −80 mV. Voltage was ramped from −120 to +45 mV within 200 ms. The inter-sweep time interval was 8 s.

The pH data were fitted using a sigmoidal and mono-exponential fit (for the homodimers) and a double sigmoidal fit (for the heterodimer) in Origin 2016. To see whether the experimentally derived pH curve is caused by a heteromerization of TREK-1 and TASK-4 or by a mixture of the homomeric currents, we calculated a theoretical, intermediate pH curve from the pH data of the homomers. For that, the sigmoidal and mono-exponential functions, used to fit the pH data of the homomeric TREK-1 and TASK-4 channels, were added, taking the injection ratio (1:1) into consideration:

$$Y(x) = \frac{1}{2} * \left(START + (END - START) * \frac{x^n}{(k^n + x^n)} \right) + \frac{1}{2} * \left(A1 * e^{\frac{-x}{t1}} + y0 \right)$$

Temperature sensitivity recordings were performed by using the TC-10/20 temperature controller (npi) in combination with the HPT-2A heated perfusion tube (ALA Scientific Instruments) and the TS-200 miniature thermistor probe (npi) in the recording chamber. This allowed for the precise heating of the bath solution to the desired temperature value. Temperature-dependent current changes were continuously recorded in a range between 15°C and 35°C using the ramp protocol mentioned above. Differences in temperature sensitivity between homodimers and heterodimers were quantified and compared by calculating the temperature coefficient (Q_{10} value) for different temperature ranges (I_1 is the recorded current amplitude at the temperature T_1, and I_2 is the recorded current amplitude at the temperature T_2):

$$Q_{10} = \frac{I_2}{I_1}^{\frac{10^\circ C}{T_2 - T_1}}$$

Drug-induced channel modulation was analysed by recording current changes after application of the different substances.

Measurements of the extracellular sodium sensitivity were performed by substituting the 96 mM NaCl in the ND96 solution with NMDG-Cl (Sigma) and analysing the changes in current after switching the solutions.

GPCR-mediated channel modulation was measured by co-expression of the desired GPCRs and subsequent stimulation with the corresponding agonist. After injection, the oocytes were incubated in theophylline-free AB solution. Due to the characteristic current run-up of TREK-1 and the slow wash-in kinetics of orforglipron, we performed run-up corrections for these experiments by washing in the modulators for 5 min and subtracting the data from non-specific, modulator-independent current changes of control measurements. The adrenoceptor agonist noradrenaline and the GLP-1 receptor agonist orforglipron were dissolved in DMSO, and the compounds were diluted in the ND96 recording solution before measurements.

For swelling experiments, the hypotonic solution was prepared by diluting ND96 solution by 50% (ND48; 104.7 mOsm·L^{-1}). For the hypertonic solution, the osmolarity of ND48 was adjusted to 434 mOsm·L^{-1} by adding saccharose. Before the swelling experiments, oocytes were preincubated in the hyperosmolar solution for 2 min. Oocytes were kept in a theophylline-free AB solution.

2.4 | Inside-out macropatch recordings

Giant patch recordings were performed with excised membrane patches from *Xenopus laevis* oocytes in the inside-out configuration at room temperature (20°C–22°C). Measurements were performed 2–3 days after cRNA injection. For the TREK-1 homodimer, a total cRNA amount of 0.5–5 ng was injected per oocyte, whereas for the TREK-1/TASK-4 heterodimer, 7.5 + 37.5 ng was used. Pipettes were pulled from thick-walled borosilicate glass capillaries (BF200-100-10, Science Products), had resistances of 0.5–1.5 MΩ and were filled with a pipette solution containing (in mM): 120 KCl, 10 HEPESand 1.0 $CaCl_2$; (pH 7.2). The bath solution applied to the intracellular side of the membrane patch had the following composition (in mM): 100 KCl, 10 HEPES and, 10 EGTA; (pH 7.2). Currents were recorded with an Axopatch 200B amplifier (Molecular Devices) and a Digidata 1550B A/D converter (Molecular Devices) at a sampling rate of 15 kHz and a filter frequency of 5 kHz. To analyse differences in the mechanosensitivity of the TREK-1 homodimer and the TREK-1/TASK-4 heterodimer, short negative pressure pulses of 2, 5, 9 and 13 cmH_2O were applied during a 10 s- long +40 mV voltage step from a holding potential of 0 mV using a U-tube manometer. At the end of the experiments, the integrity of the membrane patch was confirmed by washing in 1 mM of the intracellular pore blocker tetrapentylammonium chloride (TPA-Cl). For current analysis, data was were subsequently filtered with a 3 dB, 8-pole Bessel filter at 2 kHz. Stretch-dependent channel activation was calculated by comparing the peak current during the pressure pulse to the current before, and during the +40 mV voltage step.

2.5 | Quantification of surface expression

An extracellular haemagglutinin (HA) tag followed and preceded by a PGG sequence was introduced into human TASK-4 and TREK-1, at

14765381, 0, Downloaded from https://bpspubs.onlinelibrary.wiley.com/doi/10.1111/bph.70698 by Karlsruher Institut Fur Technologie, Wiley Online Library on [16/11/2026]. See the Terms and Conditions (https://onlinelibrary.wiley.com/terms-and-conditions) on Wiley Online Library for rules of use; OA articles are governed by the applicable Creative Commons License

amino acid positions 214 and 281, respectively. The surface expression of HA-tagged channel constructs was analysed in *Xenopus laevis* oocytes 48 h after cRNA injection. In order to block non-specific binding of antibodies, oocytes were incubated in ND96 solution supplemented with 1% (w/v) bovine serum albumin (BSA) at 4°C for 30 min. Then, oocytes were incubated for 1 h at 4°C with rat anti-HA antibodies (Roche, clone 3F10, 11867423001, RRID:AB_390918), washed at 4°C with 1% BSA/ND96 for 30 min and then incubated for 30 min at 4°C with peroxidase-conjugated secondary anti-rat antibodies (Dianova, 112-036-062, RRID:AB_2338142). Finally, oocytes were washed for 1 h at 4°C in 1% BSA/ND96 and for 15 min in ND96 solution. The chemiluminescence of single oocytes was measured as relative light units (RLUs) using SuperSignal ELISA Femto solution (Pierce) and a luminometer (Promega). Non-injected oocytes served as a negative control.

2.6 | Immunofluorescence

Our analysis of human tissue samples was approved by the Ethics Committee of the Goethe University, University Hospital Frankfurt (Approval No. 116/14). Post-mortem tissue samples from the human atrioventricular node region were fixed in a formaldehyde-based fixative and embedded in paraffin using standard procedures. Sections (5 µm) were cut on a rotary microtome, mounted on gelatin-coated slides, dried and stored at 4°C.

Pancreatic sections from slaughtered 3-month-old female domestic pigs (*Sus scrofa domestica*), were processed as described previously (Schäfer et al., 2013). Double immunofluorescence staining on FFPE sections was performed as described previously (Schäfer et al., 2013). After deparaffinization and blocking, primary antibodies against human TREK-1 (guinea pig, 1:100; APC-047-GP, Alomone Labs, RRID:AB_2756611) and human TASK-4 (rabbit, 1:100; ab198043, Abcam, RRID:AB_2933454) were co-applied in PBS/1% BSA and incubated overnight at 16°C, followed by a 2 h hour incubation at 37°C.

After extensive washing with distilled water and PBS, TREK-1 immunoreactivity was visualized using Alexa 488- conjugated donkey anti- guinea pig IgG (H + L) (Jackson ImmunoResearch, RRID: AB_2340472) diluted 1:200 in 1% BSA/PBS and incubated for 2 h at 37°C. TASK-4 immunoreactivity was detected via a two-step process: biotin-SP AffiniPure donkey anti-rabbit IgG (H + L) (Jackson ImmunoResearch, RRID:AB_2340593) diluted 1:200 in 1% BSA/PBS and incubated for 45 min at 37°C, followed by a tyramide signal amplification (TSA) step for 10 min at room temperature using an indirect tyramide reagent pack (SAT700, PerkinElmer, Rodgau, Germany) and visualization with CyTM3-conjugated streptavidin (MoBiTec, Göttingen, Germany) diluted 1:200 and incubated for 2 h at 37°C. Fluorescent signals were documented using an Olympus BX63 fluorescence microscope with a Moment-CMOS-camera (Evident, Hamburg, Germany) and Cellsense Software version 2.3. The Immuno-related procedures used comply with the recommendations made by the British Journal of Pharmacology (Alexander et al., 2018).

2.7 | Experimental design and statistical analysis

The data comply with the recommendations of the *British Journal of Pharmacology* on experimental design and analysis in pharmacology (Curtis et al., 2025). All values are expressed as means ± SEM. For all oocyte experiments, the reported group size is the number of individual oocytes recorded (n), indicated within the figures. Technical replicates in the form of recordings from the same cell were not conducted nor used for statistical analysis. n ≥ 2 different batches of oocytes were used. Data sets with n < 5 recorded oocytes were not considered for statistical analysis. The sample size was not predetermined, and the number of required experiments was estimated based on previous experiments and publications within this field. Electrophysiological oocyte recordings, that displayed no channel-specific currents or exhibited substantial leak currents (>10% of the current measured at the depolarizing current step to +40 mV), were excluded from further analysis. No exclusion criteria for outliers were established. With regard to the experiments, no randomization or blinding was performed as the different channel compositions were clearly identifiable and assignable based on current amplitude and current characteristics. To account for inter-batch heterogeneity, current amplitude and ELISA assay data were normalized to the respective homomeric control group and displayed as relative current. The percentual current change (ΔI) was calculated as follows:

$$\Delta I(\%) = \left(\frac{I_{end}}{I_{start}} - 1\right) \times 100$$

The statistical significance of the differences between group means was determined through the application of different inferential statistical test depending on the distribution of the datasets and their equality of variance. Normality was tested using the Shapiro-Wilk test. This was followed by either the parametric Levene's test or the non-parametric Brown-Forsythe test to assess the equality of variance. In case of equal variances, either the parametric two-sided Student's t-test or the non-parametric Mann–Whitney U-test was utilized. For datasets with significantly different variances, the parametric two-sided Welch's t-test or Mood's median test was employed. In cases, in which one experimental condition was tested against multiple other conditions, we have implemented the Bonferroni correction. The statistical analysis was performed using Microsoft Excel 2021 and OriginPro 2016. The respective graphs illustrate the number of replicates (n) from distinct samples. A P value < 0.05 was set as the threshold for statistical significance.

2.8 | Materials

The drugs used in this work were purchased from the following suppliers: fluoxetine from LKT (St. Paul, MN, USA), arachidonic acid from Cayman Chemicals (Ann Arbor, MI, USA) and NS-3623 from Tocris Bioscience (Minneapolis, MN, USA). Sigma-Aldrich (Taufkirchen, Germany) supplied BL-1249, chlorpromazine HCl, PD-118057, forskolin, noradrenaline HCl, propafenone HCl and verapamil HCl. IBMX

14765381, 0, Downloaded from https://bpspubs.onlinelibrary.wiley.com/doi/10.1111/bph.70698 by Karlsruher Institut Fur Technologie, Wiley Online Library on [16/11/2026]. See the Terms and Conditions (https://onlinelibrary.wiley.com/terms-and-conditions) on Wiley Online Library for rules of use; OA articles are governed by the applicable Creative Commons License

was supplied by abcr (Karlsruhe, Germany). All pharmacological modulators were initially dissolved in DMSO. Before the measurements, the stocks were diluted in ND96 recording solution, to provide the desired final concentrations and set to the desired pH value when needed. Final DMSO content did not exceed 0.5%.

2.9 | Nomenclature of Targets and Ligands

Key protein targets and ligands in this article are hyperlinked to corresponding entries in http://www.guidetopharmacology.org, and are permanently archived in the Concise Guide to PHARMACOLOGY 2025/26 (Alexander, Davenport, et al., 2025; Alexander, Gibb et al., 2025; Alexander, Striessnig, et al., 2025).

3 | RESULTS

3.1 | TASK-4 and TREK-1 are co-expressed in native tissues

The K_{2P} channels TREK-1 and TASK-4 are both expressed in the heart and pancreatic beta-cells (Blodgett et al., 2015; Hivelin et al., 2016). We re-examined these findings in tissue sections of PFA-fixed paraffin-embedded (FFPE) post-mortem human heart (Figure 1a, upper panels; Figure S1) and in porcine pancreas (Figure 1a, lower panels; Figure S2) using TREK-1- and TASK-4-specific antibodies. Double immunofluorescence staining revealed co-localization in both tissues (Figure 1a). In the pancreas, co-localization was observed predominantly in beta-cells. Based on these findings, we then hypothesized that these two channels may form heterodimers. To our knowledge, this possibility has not been investigated previously, most likely because of their distant relatedness.

3.2 | TASK-4 and TREK-1 channel subunits form functional heterodimers

Using the *Xenopus* oocyte expression system, we expressed TREK-1 alone or co-expressed TREK-1 with TASK-4, resulting in strongly diminished current amplitudes in a concentration-dependent manner (Figure 1b,c). As expected at pH 7.5, the alkaline-activated TASK-4 channel generates almost no currents. However, its co-expression strongly reduced TREK-1 currents (Figure 1b,c). Thus, as a control to show functional expression, TASK-4 was measured at a more alkaline pH (pH 9), revealing robust current amplitudes (Figure 1c). In addition, the complete TREK-1/TASK-4 co-expression experiments described above were subsequently performed at more alkaline conditions (pH 9). Again, co-expression of TREK-1 with TASK-4 resulted in a concentration-dependent current decrease, even at a pH at which TASK-4 channels generate larger macroscopic currents (Figure 1d).

Next, we examined the plasma membrane expression of the heterodimers compared to each channel expressed alone (Figure 1e,f). In this chemiluminescence-based ELISA assay, extracellular haemagglutinin (HA-Ex)-tagged channel constructs were used to exclusively quantify the channels at the cell surface. Co-expression of TASK-$4^{HA\text{-}Ex}$ with non-tagged TREK-1 markedly reduced the membrane expression of TASK-$4^{HA\text{-}Ex}$ (Figure 1e). Similarly, co-expression of TREK-$1^{HA\text{-}Ex}$ with non-tagged TASK-4 also led to a reduced TREK-$1^{HA\text{-}Ex}$ channel abundance at the plasma membrane (Figure 1f). These data suggest that heterodimers are less efficiently transported to the plasma membrane, when compared with the respective homodimers. For a direct comparison of current amplitudes to surface expression, we repeated the co-expression analysis in voltage-clamp experiments, using the identical cRNA amounts as used in the chemiluminescence assays (Figure 1f vs. g). The co-expression-dependent current decrease was more pronounced than the reduction in surface expression (Figure 1f,g). This indicates that the heteromerization-dependent current reduction does not only result from altered membrane trafficking but also points towards changes in the channel gating.

Co-expression studies utilizing selectivity filter defect channel mutants that act in a dominant-negative manner are a widely used approach to probe for heteromerization of potassium channels (Khoubza et al., 2022; Levitz et al., 2016; Rinné et al., 2024). Here, the highly conserved GYG motif within the pore signature sequence of K_{2P} channels is changed to EYG. In our experiments, co-expression of such a non-conducting TASK-4^{G118E} construct markedly reduced the TREK-1 current amplitude, recorded at pH 7.5 (Figure 1h,i). As a control, TASK-4^{WT} was co-expressed with the dominant-negative TASK-4^{G118E} pore mutant, which resulted in a pronounced current reduction, as expected for homodimerization (Figure 1j). These measurements were performed at pH 10.5 to record large macroscopic TASK-4 currents. Conversely, co-expression of TREK-1^{G159E} with TASK-4^{WT} also reduced TASK-4 currents (Figure 1j). From these experiments, we concluded that TREK-1 and TASK-4 form functional heterodimers at the plasma membrane.

3.3 | TREK-1/TASK-4 heterodimers display unique gating properties to physiological stimuli

To confirm and elaborate on our findings that the heteromeric TREK-1/TASK-4 channels have altered gating, we performed experiments analysing the characteristic features of both channels. In terms of the temperature sensitivity, TREK-1 currents increased with rising temperatures, as expected, whereas TASK-4 was not temperature sensitive (Figure 2a). Co-expression of both channels resulted in unique changes in the temperature sensitivity compared to TREK-1, depending on the temperature range (Figure 2a,b). While co-expression with TASK-4 decreased the Q_{10} value compared to TREK-1 in the range of moderate cold temperatures (15°C–20°C), there was no significant change in temperature sensitivity in the range of 20°C–25°C (Figure 2b). Strikingly, we found at higher temperatures that the heterodimeric TREK-1/TASK-4 channels have an elevated temperature sensitivity compared to homomeric TREK-1 channels (Figure 2a,b). Thus, TASK-4 co-expression significantly amplifies the temperature

14765381, 0, Downloaded from https://bpspubs.onlinelibrary.wiley.com/doi/10.1111/bph.70698 by Karlsruher Institut Fur Technologie, Wiley Online Library on [16/11/2026]. See the Terms and Conditions (https://onlinelibrary.wiley.com/terms-and-conditions) on Wiley Online Library for rules of use; OA articles are governed by the applicable Creative Commons License

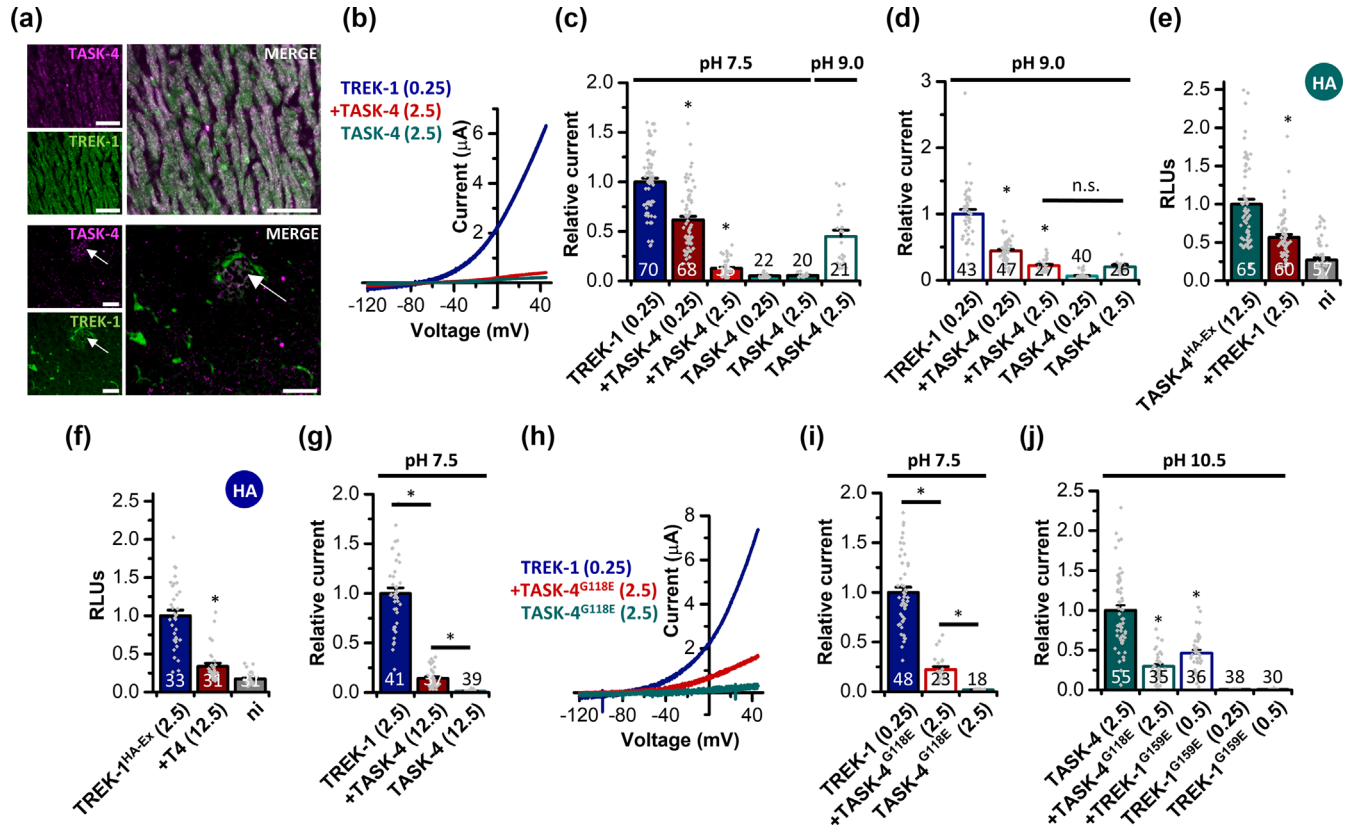


FIGURE 1 TASK-4 and TREK-1 channel subunits form functional heterodimers. (a) Representative double immunofluorescence staining of TASK-4 and TREK-1 in cardiac and pancreatic tissue sections showing co-localization in both tissues with co-localized signals in white false colour. Upper panels: FFPE post-mortem section of the human AV nodal region. Lower panels: FFPE section of porcine pancreas. Scale bars indicate 50 µm. (b) Representative current traces of TREK-1 (blue), TASK-4 (green) or TREK-1 co-expressed with TASK-4 (red) recorded at pH 7.5 in *Xenopus* oocytes using a voltage-ramp protocol. (c, d) Current amplitudes analysed at +40 mV of TREK-1 and TASK-4 expressed alone or co-expressed in a 1:1 and 1:10 ratio, recorded in oocytes at pH 7.5 or pH 9, as indicated. (e) Quantification of the extracellular haemagglutinin-tagged TASK-4$^{HA\text{-}Ex}$ surface expression in a chemiluminescence-based ELISA assay alone (green) or when co-expressed with TREK-1 (red), measured in relative light units (RLUs). Un-injected oocytes (ni) (grey) served as a negative control. (f) Quantification of TREK-1$^{HA\text{-}Ex}$ surface expression in a chemiluminescence-based ELISA assay expressed alone (blue) or when co-expressed with TASK-4 (red). (g) Relative current amplitudes of TREK-1 (blue) and TASK-4 (green) expressed alone or co-expressed (red) using the ratios and the same amounts of cRNA, as also used in the ELISA assay in panel (f), recorded at pH 7.5. (h) Representative current traces of TREK-1 (blue), the pore 'dead' mutant TASK-4^{G118E} (green) or TREK-1 co-expressed with TASK-4^{G118E} (red) recorded in *Xenopus* oocytes using a voltage-ramp protocol, recorded at pH 7.5. (i) Relative current amplitudes analysed at +40 mV and normalized to TREK-1. (j) Relative current amplitudes of TASK-4 expressed alone or co-expressed with the pore 'dead' mutants TASK-4^{G118E} or TREK-1^{G159E}, compared to TREK-1^{G159E} expressed alone. Currents were recorded at pH 10.5 and analysed at +40 mV. The data were normalized to the mean TASK-4 current amplitude. The injected amount of cRNA is provided in nanograms per oocyte in brackets. Numbers of experiments are displayed within the bars. Data presented are individual values with means ± SEM. *P < 0.05, significantly different as indicated; n.s., not significant.

responsiveness of TREK-1, particularly as it approaches and enters physiological ranges (>25°C) (Figure 2b).

Because TREK-1 channels are modulated by POPDC proteins (Froese et al., 2012), we wondered how heterodimeric TREK-1/TASK-4 channels would respond (Figure 2c,d). As described, TREK-1 current amplitude was increased upon POPDC1 co-expression, whereas TASK-4 was not modulated by POPDC1 (Figure 2d). The co-expression of TASK-4 with TREK-1 caused a significant, but somewhat less pronounced, current increase by POPDC1 (Figure 2c,d). This reduced effect was, however, not significantly smaller than the POPDC1 modulation observed for the TREK-1 homomeric channel (Figure 2c,d). Such results would be expected if one TREK-1 subunit were enough in the heteromeric channel complex to mediate the POPDC effects.

TREK-1 channels have been reported to be activated by extracellular Na^+, whereas TASK-4 channels display no such dependence on extracellular Na^+ (Figure 2e). Remarkably, the heterodimeric TREK-1/TASK-4 channels show a drastically reduced activation by extracellular Na^+, compared to TREK-1, providing strong evidence for heteromerization of the two channels.

14765381, 0, Downloaded from https://bpspubs.onlinelibrary.wiley.com/doi/10.1111/bph.70698 by Karlsruher Institut Fur Technologie, Wiley Online Library on [16/11/2026]. See the Terms and Conditions (https://onlinelibrary.wiley.com/terms-and-conditions) on Wiley Online Library for rules of use; OA articles are governed by the applicable Creative Commons License

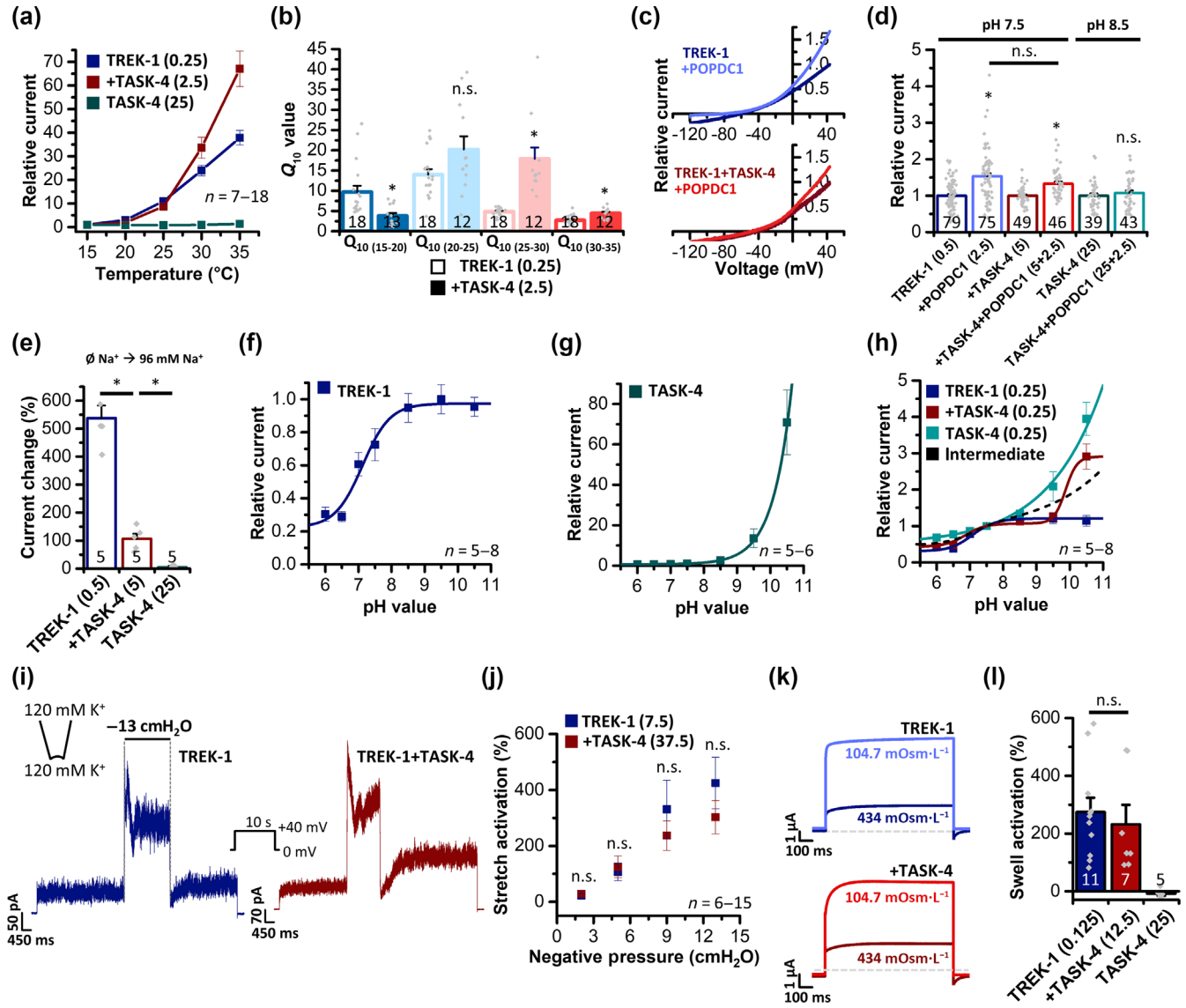


FIGURE 2 TREK-1/TASK-4 heterodimers display unique gating properties to physiological stimuli. (a) Effects of temperature changes on current amplitudes of TREK-1 (blue) or TASK-4 (green) expressed alone or when co-expressed (red) in oocytes. Recordings were normalized to current amplitudes at 15°C at +40 mV, respectively. (b) Q_{10} values at different temperature ranges for TREK-1 alone (open columns) or after co-expression with TASK-4 (filled columns). (c) Upper panel, representative current traces recorded in oocytes after expression of TREK-1 alone (dark blue) or together with POPDC1 (blue). Lower panel, representative current traces of TREK-1 co-expressed with TASK-4 with (red) or without POPDC1 (dark red). (d) Relative current amplitudes analysed at +40 mV and normalized to TREK-1 (blue), TASK-4 (green) or the current amplitude after TREK-1 and TASK-4 co-expression (red), respectively. Amplitudes are analysed in the absence and presence of POPDC1 (DC1). The pH value during the recordings is indicated above. (e) Extracellular sodium sensitivity of TREK-1 (blue) and TASK-4 (green) when expressed alone or after co-expression of both channels (red). Current activation by Na^+ was analysed after replacing NMDG-Cl with NaCl in the recording solution. (f) The pH sensitivity of TREK-1 (0.25 ng) (blue) and (g) TASK-4 (5 ng) (green) when expressed alone or (h) in comparison to the co-expression of both channel subunits (red) in a 1:1 ratio (0.25 ng for each construct). The mathematically calculated intermediate pH curve of channels that do not form heteromers is indicated as a dashed line (black). (i) Representative inside-out macropatch clamp recordings of stretch-induced currents (−13 cmH_2O column) for the TREK-1 homomeric channel (blue) and the TREK-1/TASK-4 heterodimers (red). Inset illustrates the holding potential during application of the stretch pulses. (j) Stretch sensitivity of TREK-1 when expressed alone or in comparison to the co-expression of both channel subunits in a 1:5 ratio, recorded by application of different negative pressure pulses. Recordings were normalized to current amplitudes at +40 mV, before application of the negative pressure pulses. (k) Representative current traces of swelling-induced changes in current amplitudes for both the TREK-1 homomer (blue) and TREK-1/TASK-4 heterodimer (red). Cell swelling was achieved by switching between a hypertonic ND48 solution containing saccharose and a hypotonic ND48 solution without saccharose. (l) Analyses of the swelling-induced changes in current amplitudes of TREK-1 (blue) and TASK-4 (green) alone or the heteromeric TREK-1/TASK-4 channel complex (red). The data were normalized to the current amplitudes recorded at +40 mV before application of the hypotonic ND48 solution. cRNA amounts injected are shown in nanograms per oocyte in brackets. Numbers of experiments are displayed within the bars/graphs. Data are presented as means ± SEM, with individual values. *$P < 0.05$, significantly different as indicated; n.s., not significant.

14765381, 0, Downloaded from https://bpspubs.onlinelibrary.wiley.com/doi/10.1111/bph.70698 by Karlsruher Institut Fur Technologie, Wiley Online Library on [16/11/2026]. See the Terms and Conditions (https://onlinelibrary.wiley.com/terms-and-conditions) on Wiley Online Library for rules of use; OA articles are governed by the applicable Creative Commons License

In our experiments, TASK-4 and TREK-1 channels are both sensitive to changes in extracellular pH, however, to a different extent and within different pH ranges (Figure 2f,g), similar to those previously described (Decher et al., 2001; Sandoz et al., 2009). While TASK-4 currents are drastically activated by alkalization (Figure 2g), co-expression of similar amounts of TREK-1 and TASK-4 resulted in a unique pH dependence that could be fitted using a double Hill equation (Figure 2h), which was different to that of TASK-4 or TREK-1 alone. Markedly, this unique pH dependence was different to the intermediate curve calculated for two independent, mixed pH curves (Figure 2h), again highlighting that the channels form heteromeric channel complexes.

Another characteristic feature of TREK-1 is activation upon membrane stretch, whereas TASK-4 channels are not described as stretch sensitive. To test for heteromerization-dependent changes in the mechanosensitivity compared to TREK-1, we performed inside-out macropatch clamp recordings, applying short negative pressure pulses, as well as experiments with cell swelling. In comparison to TREK-1, the co-expression with TASK-4 channels caused no significantly altered stretch sensitivity (Figure 2i,j), indicating that the heteromeric channel complexes do not have a mixed sensitivity to stretch but take over the behaviour of TREK-1. Cell swelling experiments using hypo-osmolar and hyperosmolar solutions led to similar results, as the heteromeric channel complex of TASK-4 and TREK-1 adopted the same behaviour as TREK-1 alone (Figure 2k,l).

3.4 | The putative effects of PCCD and RVOT-VT mutations on TREK-1/TASK-4 heteromers

In the heart, TASK-4 is strongly expressed in the cardiac conduction system (sinoatrial node, AV node and Purkinje fibres) (Friedrich et al., 2014). The gain-of-function mutation TASK-4^{G88R} is associated with PCCD (Friedrich et al., 2014). As TREK-1 is also expressed in these cardiac tissues (Schmidt et al., 2014; Schmidt et al., 2015; Wiedmann et al., 2021), we were interested in the effects of the TASK-4^{G88R} variant in the heterodimeric channel complex. Here, the TASK-4^{G88R} mutant led to an increase in current amplitude in the heteromeric complex with TREK-1 (Figure 3a,b), which was similar to what was observed for the TASK-4^{G88R} mutant expressed alone. Therefore, the disease-causing gain-of-function in TASK-4 also persists in the heteromeric channel complexes, and the heterodimerization does not alter this disease-causing mechanism.

Although TREK-1 is expressed in different parts of the heart, it is most abundant in ventricular tissue (Schmidt et al., 2015; Schmidt, Wiedmann, Kallenberger, et al., 2017). The TREK-1^{I267T} variant is associated with RVOT-VT (Decher, Ortiz-Bonnin, et al., 2017). These mutant channels show a current reduction, a sodium permeability and increased stretch sensitivity (Decher, Ortiz-Bonnin, et al., 2017). To test for effects of heteromerization in this pathophysiological context, we co-expressed TREK-1 or TREK-1^{I267T} with TASK-4. Interestingly, the heteromerization-induced current reduction of TREK-1 by TASK-4 was greatly attenuated for the TREK-1^{I267T} mutant

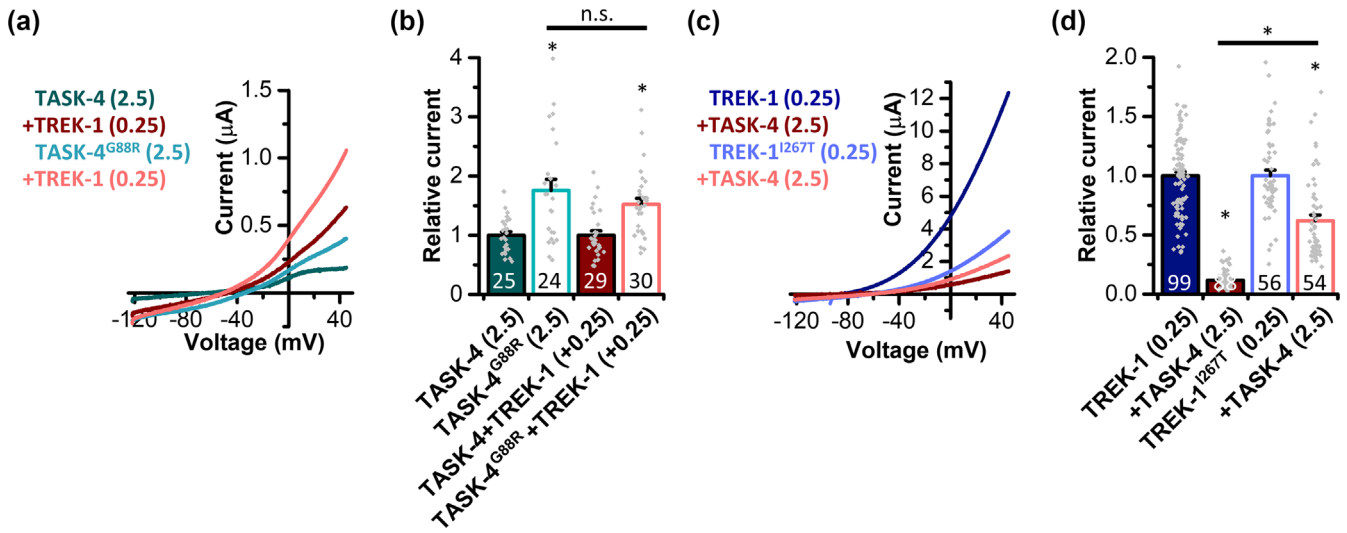


FIGURE 3 The putative effects of PCCD and RVOT-VT mutations on TREK-1/TASK-4 heteromers. (a) Representative current traces of wild-type TASK-4 (green) or TREK-1/TASK-4 heterodimeric channels (red) and TASK-4^{G88R} (light green) or TREK-1/TASK-4^{G88R} (light red) channels using a voltage-ramp protocol recorded at pH 7.5. (b) Current amplitudes of TASK-4 versus TASK-4^{G88R} expressed alone or co-expressed in a 1:10 ratio with TREK-1, recorded at pH 7.5. The data were analysed at +40 mV and normalized to TASK-4 or TREK-1/TASK-4, respectively. (c) Representative current traces of TREK-1 (blue) and TREK-1/TASK-4 (red) heterodimeric channels and TREK-1^{I267T} (light blue) and TREK-1^{I267T}/TASK-4 channels (light red) using a voltage-ramp protocol, recorded at pH 7.5. (d) Current amplitudes of TREK-1 and TREK-1^{I267T} expressed alone or co-expressed with TASK-4 in a 1:10 ratio, recorded at pH 7.5. The data were analysed at +40 mV and normalized to TREK-1 and TREK-1^{I267T}, respectively. cRNA amounts injected are illustrated in nanograms per oocyte in brackets. Numbers of experiments are displayed within the bars. Data are presented as means ± SEM, with individual values. *P < 0.05, significantly different as indicated; n.s., not significant.

14765381, 0, Downloaded from https://bpspubs.onlinelibrary.wiley.com/doi/10.1111/bph.70698 by Karlsruher Institut Fur Technologie, Wiley Online Library on [16/11/2026]. See the Terms and Conditions (https://onlinelibrary.wiley.com/terms-and-conditions) on Wiley Online Library for rules of use; OA articles are governed by the applicable Creative Commons License

(Figure 3c,d). Therefore, the significantly increased currents of heteromeric TASK-4/TREK-1^{I267T} channels compared with those of TREK-1/TASK-4 heteromers (Figure 3d) might also be of disease-causing relevance.

3.5 | TREK-1/TASK-4 heterodimer channels display a unique pharmacology

Next, we investigated whether the heteromeric TREK-1/TASK-4 channels exhibit an altered pharmacology for activators (Figure 4a–d) or blockers (Figure 4e–h). **BL-1249** caused an intermediate activation of the heteromeric channels compared to the homomeric TASK-4 and TREK-1 channels (Figure 4a). In contrast, the activation of the heteromeric channels by **NS-3623** and **arachidonic acid** was more similar to that of the TASK-4 channel expressed alone (Figure 4b,c). Notably, **PD-118057** displayed a particularly striking pharmacological signature, resulting in a diminished activation of the heteromeric TREK-1/TASK-4 channels compared to homomeric forms (Figure 4d).

Also, a distinct blocker sensitivity profile was observed for heteromeric TREK-1/TASK-4 channels. Verapamil caused an intermediate block of the heteromeric channels compared to homomeric TASK-4 or TREK-1 (Figure 4e), which is highlighted by a rightward shift of the dose–response curve and an increase in the EC_{50} value from 129 μM for the homomeric TREK-1 channel to 520 μM for the TREK-1/TASK-4 heteromeric channel (Figure S3A). In contrast, the inhibition of the heteromeric channels by **propafenone** and **fluoxetine** was more similar to that of the TREK-1 channel expressed alone (Figure 4f,g). Here, both drugs activated TASK-4 while they both blocked the heteromeric channel complex (Figure 4f,g). Thus, the SSRI fluoxetine, the active ingredient of Prozac®, also blocks heteromeric TREK-1/TASK-4 channel complexes, which is of major relevance, as TREK-1 inhibition was considered to contribute to its antidepressant mechanism of action (Kennard et al., 2005). In addition, **chlorpromazine** (100 μM), which inhibits TREK-1, but activates TASK-4, did not cause any significant changes in TREK-1/TASK-4 current amplitudes (Figure 4h). Interestingly, the dose–response curve of the heteromeric TREK-1/TASK-4 channel complex revealed a loss of drug sensitivity up to 250-μM

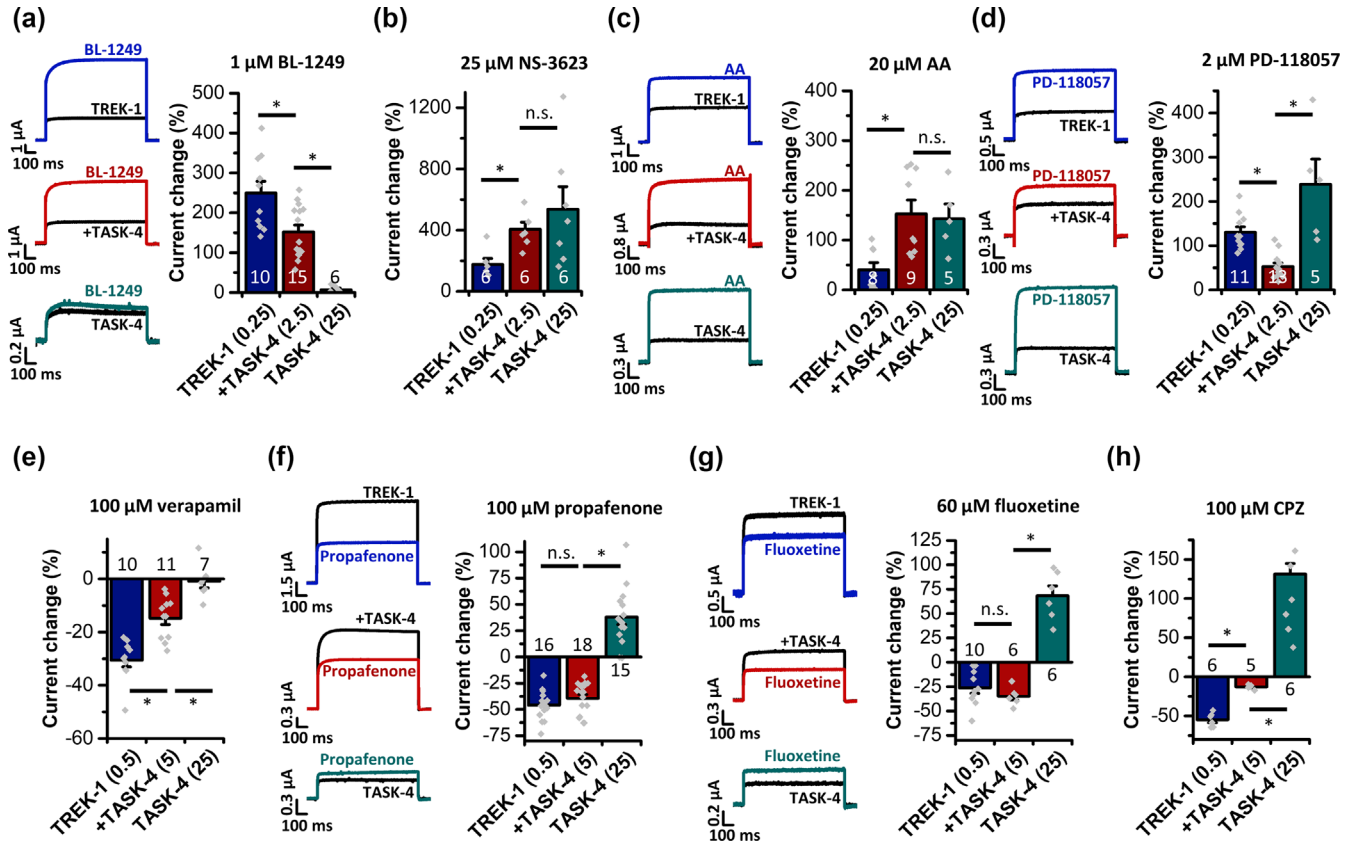


FIGURE 4 TREK-1/TASK-4 heterodimer channels display a unique pharmacology. (a) Analysis of the effect of the TREK-1 activators BL-1249 (1 μM), (b) NS-3623 (25 μM), (c) arachidonic acid (AA) (20 μM) or (d) PD-118057 (2 μM) on the current amplitudes of TREK-1 (blue), TASK-4 (green) or TREK-1 co-expressed with TASK-4 (red). Changes in current amplitudes were analysed at +40 mV. (a, c, d) Representative current traces before and after application of the indicated substances. (e) Analysis of the effect of the TREK-1 inhibitors verapamil (100 μM), (f) propafenone (100 μM), (g) fluoxetine (60 μM) or (h) chlorpromazine (CPZ) (100 μM) on the current amplitudes of TREK-1 (blue), TASK-4 (green) or TREK-1 co-expressed with TASK-4 (red). Changes in current amplitudes were analysed at +40 mV. (f–h) Representative current traces before and after application of the indicated substances. cRNA amounts injected are provided in nanograms per oocyte in brackets. Numbers of experiments are displayed within the bars. Data are presented as mean ± SEM, with individual values. *P < 0.05, significantly different as indicated; n.s., not significant.

14765381, 0, Downloaded from https://bpspubs.onlinelibrary.wiley.com/doi/10.1111/bph.70698 by Karlsruher Institut Fur Technologie, Wiley Online Library on [16/11/2026]. See the Terms and Conditions (https://onlinelibrary.wiley.com/terms-and-conditions) on Wiley Online Library for rules of use; OA articles are governed by the applicable Creative Commons License

chlorpromazine, whereas higher concentrations resulted in an activation of the heteromeric channel complex (Figure S3B).

Taken together, these data strongly suggest that TREK-1/TASK-4 form heterodimers with a unique pharmacological profile that must be considered in future experimental studies and drug development.

3.6 | TASK-4 heterodimerization with TREK-1 attenuates G_S receptor coupling and PKA regulation of TREK-1

TREK-1 channels are inhibited upon G_S receptor activation via a PKA-dependent channel phosphorylation (Murbartian et al., 2005). In contrast, TASK-4 channels are not functionally coupled to G_S receptors. Therefore, we examined the receptor coupling of the heteromeric TREK-1/TASK-4 channel complexes, using different approaches (Figure 5). First, we expressed TREK-1, TASK-4 or both channel subunits together with the β_1 **adrenoceptor** and applied **noradrenaline** (500 nM) to stimulate the receptor. In TREK-1-expressing oocytes, the receptor activation led to channel inhibition, whereas homomeric TASK-4 currents were slightly activated (Figure 5a,b). Strikingly, upon β_1 adrenoceptor activation, no effect on current amplitudes was observed for the heteromeric TREK-1/TASK-4 channel complex (Figure 5a,b). We next examined whether similar effects could be observed upon co-expression and activation of the **GLP-1 receptor** by **orforglipron** (1 μM). In line with the altered β_1 adrenoceptor signalling, activation of the GLP-1 receptor inhibited TREK-1 and modestly activated homomeric TASK-4 currents, whereas heteromeric TREK-1/TASK-4 channels remained insensitive (Figure 5a–c).

To analyse the mechanism of this impaired G_S-mediated coupling of the heterodimeric TREK-1/TASK-4 channel complex, we applied the **adenylyl cyclase** activator **forskolin** together with the phosphodiesterase inhibitor **IBMX** to increase cAMP levels and subsequently PKA activity. As previously described, a phosphorylation-dependent reduction in TREK-1 current amplitude was observed. Strikingly, however, TREK-1/TASK-4-expressing oocytes were insensitive to changes in PKA levels (Figure 5d,e). Thus, the lack of a G_S-receptor-coupled inhibition of the heteromeric channel complex is due to a loss of a PKA-dependent channel inhibition.

Accordingly, our findings suggest that altered TREK-1 receptor coupling, along with the distinct pharmacology of the TREK-1/TASK-4 heterodimer, may be physiologically relevant and has important implications for the development of antiarrhythmic, antidiabetic and antidepressant therapies.

4 | DISCUSSION

Here, we describe our experiments showing that TASK-4 and TREK-1 channels form heteromeric channel complexes with distinct functional features, characterized by altered pH and sodium dependence, temperature gating, a unique pharmacology and a strongly altered G-protein receptor coupling. While heteromerization was initially thought to be restricted to members of the same subfamily, recent studies have begun to uncover interactions between different subfamilies (Khoubza et al., 2021). The distinct co-distribution of TREK-1 and TASK-4 in the heart and pancreas, together with their shared involvement in inherited cardiac arrhythmias, prompted us to

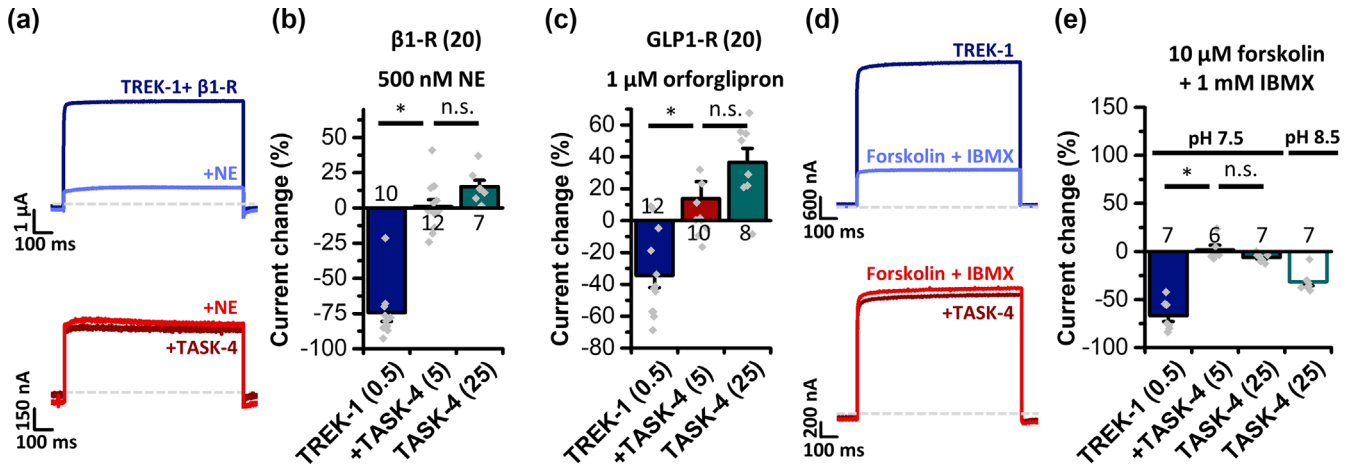


FIGURE 5 TASK-4 heterodimerization with TREK-1 attenuates G_S receptor coupling and PKA regulation of TREK-1. (a) Representative current traces before and after application of 500 nM noradrenaline (NE) on oocytes co-expressing TREK-1 plus β_1-adrenoceptor (blue) or TASK-4 plus β_1-adrenoceptor (red). (b) Mean G_s-mediated current changes after application of 500-nM NE on TREK-1 (blue), TASK-4 (green) or TREK-1 co-expressed with TASK-4 (red). Currents were recorded at pH 7.5 and analysed at 0 mV. (c) Mean G_s-mediated current changes by 1-μM orforglipron for the human GLP-1 receptor co-expressed with TREK-1 (blue), TASK-4 (green) or TREK-1 co-expressed with TASK-4 (red). The data were recorded at pH 7.5 and analysed at +40 mV. (d) Representative current traces before and after application of 1-μM forskolin and 1-mM IBMX on oocytes expressing TREK-1 (blue) or co-expressing TREK-1 and TASK-4 (red). (e) Current changes by 1-μM forskolin and 1 mM IBMX for oocytes expressing TREK-1 (blue), TASK-4 (green) or TREK-1 plus TASK-4 (red). The injected amount of cRNA is provided in nanograms per oocyte in brackets. Numbers of experiments are displayed within the bars. Data are presented as means ± SEM, with individual values. *$P < 0.05$, significantly different as indicated; n.s., not significant.

14765381, 0, Downloaded from https://bpspubs.onlinelibrary.wiley.com/doi/10.1111/bph.70698 by Karlsruher Institut Fur Technologie, Wiley Online Library on [16/11/2026]. See the Terms and Conditions (https://onlinelibrary.wiley.com/terms-and-conditions) on Wiley Online Library for rules of use; OA articles are governed by the applicable Creative Commons License

investigate whether these channels form functional heteromeric channel complexes. Such interaction was initially unexpected, as both subunits belong to different subfamilies with highly distinct functional hallmarks. The co-assembly of these channel subunits is a compelling example of heteromerization across subfamilies, a finding that also reveals K_{2P} channels to be far more promiscuous than their formal classification suggests. The current study also suggests that such unconventional combinations provide fundamental mechanisms to diversify the electrical repertoire of normal tissues and that there is a need to study heterodimerization in a more tissue-oriented manner, than by family conservation alone. The presence of TREK-1/TASK-4 heterodimers in the heart and pancreas offers a new perspective on the clinical phenotypes and pathophysiological mechanisms previously associated with mutations in either of the channels alone. For instance, the increased currents of heteromeric TREK-1^{I267T}/TASK-4 channels compared to the TREK-1/TASK-4 heteromers might contribute to the disease-causing mechanism, suggesting that the pathophysiology of the reported case of inherited RVOT-VTs may not only stem from homomeric TREK-1 channel dysfunction.

Another major finding of this study is the significantly altered temperature sensitivity of the TREK-1/TASK-4 heterodimers. While for the channels of the TREK subfamily, including TREK-1, TREK-2 and **TRAAK**, a role in thermosensation is well established (Kang et al., 2005; Maingret et al., 2000; Viatchenko-Karpinski et al., 2018), TASK-4 homomeric channels show no temperature sensitivity and therefore have never been studied as putative modulators of thermosensitivity in the nervous system. Another reason for a lack of studies in this field is that *KCNK17*, encoding TASK-4, is not expressed in mice, the most widely used model organism in sensory physiology. However, our data suggest that the assembly of TASK-4 with TREK-1 leads to a channel complex with an amplified temperature response, particularly as the temperature enters the physiological range (>25°C). Interestingly, we detected a robust expression of TASK-4 transcripts in human skin samples by RT-PCR (not illustrated), a finding that is consistent with recent transcriptomic data (Zhu et al., 2023). Because TREK-1 was previously described in human skin (Kang et al., 2007), a putative heterodimerization of these channels might contribute to thermal perception or thermoregulation in humans. Here, by shifting the temperature sensitivity threshold at physiological temperatures, the heteromerization with TASK-4 channel subunits may fine-tune TREK-1 to be a more efficient temperature sensor in human peripheral tissue.

The unique pharmacological profile of TREK-1/TASK-4 heterodimers is of major clinical significance, particularly for the development of drugs targeting these channels in cardiac and pancreatic tissue. The TREK-1/TASK-4 heterodimerization preserves or even enhances the characteristic features of TREK-1 channel, such as the inhibition by fluoxetine (Prozac), the activation by arachidonic acid, the stretch activation and the temperature sensitivity, whereas the response to other modulators is strongly altered. For instance, the efficacy of TASK-4 activators, such as chlorpromazine, is markedly reduced in the heteromeric complex. This indicates distinct drug accessibility and/or binding sites for the heteromeric channel complexes. These findings highlight a significant translational obstacle, because drugs that are optimized against homomeric channels to treat a particular pathological condition, may fail to achieve their intended effects in normal tissues, where the TREK-1/TASK-4 heterodimers are present. Therefore, the effects on TREK-1/TASK-4 heteromers must be considered, in order to allow for off-target effects or failures in clinical studies, as a result of altered potency *in vivo*.

Most importantly, the TREK-1/TASK-4 heterodimers display attenuated G_s-coupled receptor signalling and PKA-dependent regulation, which is a characteristic feature of homomeric TREK-1 channels. In pancreatic beta-cells, this may have significant implications for the incretin pathway. Incretins, such as GLP-1 also signal via G_s and PKA pathways to modulate insulin secretion (Lymperopoulos et al., 2025). Our data suggest that while homomeric TREK-1 is typically inhibited by PKA, the TREK-1/TASK-4 complex maintains its conductance under these conditions. This sustained, GLP-1-independent, potassium leak conductance may prevent excessive depolarization and may stabilize calcium oscillations, thereby refining the electrical bursting patterns required for efficient insulin secretion. This mechanism suggests that the heterodimer acts as a key modulator of the incretin effect, ensuring that the beta-cell response remains finely balanced. A similar theory may apply to the cardiac conduction system, specifically the AV node, where TREK-1 and TASK-4 are highly expressed. Under strong sympathetic stimulation (e.g., via β-adrenoceptors), homomeric TREK-1 channels would undergo near-complete inhibition. However, the presence of TREK-1/TASK-4 heterodimers with reduced PKA sensitivity would grant a repolarization reserve. This might prevent the AV node from becoming over-excitable during adrenergic stress, allowing for a more precise fine-tuning of AV conduction. Thus, the heteromerization of TASK-4 and TREK-1 appears to be a functional strategy to 'buffer' GPCR-triggered responses in specific tissues.

In conclusion, our findings demonstrate that the interaction between TASK-4 and TREK-1 modulates key channel properties, ranging from pH sensing to receptor coupling, thereby establishing these heterodimers as functionally distinct players in cardiac and pancreatic physiology. Our results emphasize the therapeutic relevance of K_{2P} heterodimerization, highlighting that future drug development must account for the unique pharmacological and regulatory signatures of the TREK-1/TASK-4 channel complex.

AUTHOR CONTRIBUTIONS

Sven Schütte: Investigation; formal analysis; writing—review and editing; writing—original draft. **Florian Schick:** Writing—review and editing; investigation; formal analysis. **Emilia De Martino:** Investigation; formal analysis; writing—review and editing. **Hannah Schmitz:** Writing—review and editing; investigation. **Katharina E.S. Zander:** Investigation; writing—review and editing. **Franziska Holz:** Investigation; writing—review and editing. **Patrick Sauer:** Investigation; writing—review and editing. **Luise Mildeberger:** Investigation; writing—review and editing. **Moritz Linder:** Investigation; writing—review and editing; formal analysis. **Axel Loewe:** Writing—review and editing; formal analysis. **Aytug K. Kiper:** Investigation; writing—review and editing; formal analysis. **Silke Kauferstein:** Investigation; writing—review and editing. **Martin**

14765381, 0, Downloaded from https://bpspubs.onlinelibrary.wiley.com/doi/10.1111/bph.70698 by Karlsruher Institut Fur Technologie, Wiley Online Library on [16/11/2026]. See the Terms and Conditions (https://onlinelibrary.wiley.com/terms-and-conditions) on Wiley Online Library for rules of use; OA articles are governed by the applicable Creative Commons License

K.-H. Schäfer: Investigation; writing—review and editing; validation. **Susanne Rinné:** Investigation; writing—review and editing; formal analysis; supervision; data curation; writing—original draft. **Niels Decher:** Conceptualization; investigation; writing—review and editing; writing—original draft; funding acquisition; project administration; supervision; resources.

ACKNOWLEDGEMENTS

We thank Simone Preis for expert technical assistance. The study was supported by Deutsche Forschungsgemeinschaft DE1482/9-1 (to ND), Studienstiftung des deutschen Volkes (to SS) and Medizinstiftung der Philipps-Universität Marburg (to FS). Open Access funding enabled and organized by Projekt DEAL.

CONFLICT OF INTEREST STATEMENT

The authors declare no conflicts of interest.

DATA AVAILABILITY STATEMENT

The data that support the findings of this study are available from the corresponding author upon reasonable request. Some data may not be made available because of privacy or ethical restrictions.

DECLARATION OF TRANSPARENCY AND SCIENTIFIC RIGOUR

This Declaration acknowledges that this paper adheres to the principles for transparent reporting and scientific rigour of preclinical research as stated in the *BJP* guidelines for Design and Analysis, Immunoblotting and Immunochemistry, and Animal Experimentation and as recommended by funding agencies, publishers and other organizations engaged with supporting research.

ORCID

Sven Schütte https://orcid.org/0009-0009-9867-2799
Florian Schick https://orcid.org/0009-0002-9393-6934
Emilia De Martino https://orcid.org/0009-0004-7663-7195
Hannah Schmitz https://orcid.org/0009-0008-0854-9985
Katharina E. S. Zander https://orcid.org/0009-0003-9054-2267
Patrick Sauer https://orcid.org/0009-0006-2307-5234
Luise Mildeberger https://orcid.org/0000-0002-7453-4078
Moritz Linder https://orcid.org/0009-0000-1228-159X
Axel Loewe https://orcid.org/0000-0002-2487-4744
Aytug K. Kiper https://orcid.org/0000-0003-2850-2523
Silke Kauferstein https://orcid.org/0000-0003-0066-8679
Martin K.-H. Schäfer https://orcid.org/0009-0009-3554-2356
Susanne Rinné https://orcid.org/0000-0003-2326-7069
Niels Decher https://orcid.org/0000-0001-8892-1231

REFERENCES

Alexander, S. P. H., Davenport, A. P., Kelly, E., Gibb, A. J., Mathie, A. A., Peach, C. J., Veale, E. L., Armstrong, J. F., Faccenda, E., Harding, S. D., Southan, C., Davies, J. A., Abbracchio, M. P., Abraham, G. R., Agoulnik, A., Alexander, W., Al-Hosaini, K., Bäck, M., Baker, J. G., … Zaidman, N. (2025). The concise guide to PHARMACOLOGY 2025/26: G protein-coupled receptors. *British Journal of Pharmacology*, *182*(Suppl 1), S24–S151.

Alexander, S. P. H., Gibb, A. J., Kelly, E., Mathie, A. A., Peach, C. J., Veale, E. L., Armstrong, J. F., Faccenda, E., Harding, S. D., Southan, C., Davies, J. A., Amarosi, L., Anderson, C. M. H., Beart, P. M., Broer, S., Dawson, P. A., Gyimesi, G., Hagenbuch, B., Hammond, J. R., … Verri, T. (2025). The Concise Guide to PHARMACOLOGY 2025/26: Transporters. *British Journal of Pharmacology*, *182*(Suppl 1), S404–S496. https://doi.org/10.1111/bph.70235

Alexander, S. P. H., Roberts, R. E., Broughton, B. R. S., Sobey, C. G., George, C. H., Stanford, S. C., Cirino, G., Docherty, J. R., Giembycz, M. A., Hoyer, D., Insel, P. A., Izzo, A. A., Ji, Y., MacEwan, D. J., Mangum, J., Wonnacott, S., & Ahluwalia, A. (2018). Goals and practicalities of immunoblotting and immunohistochemistry: A guide for submission to the *British Journal of Pharmacology*. *British Journal of Pharmacology*, *175*(3), 407–411.

Alexander, S. P. H., Striessnig, J., Gibb, A. J., Mathie, A. A., Veale, E. L., Kelly, E., Peach, C. J., Armstrong, J. F., Faccenda, E., Harding, S. D., Southan, C., Davies, J. A., Aldrich, R. W., Attali, B., Baggetta, A. M., Becirovic, E., Beech, D. J., Biel, M., Bill, R. M., … Zhu, M. (2025). The concise guide to PHARMACOLOGY 2025/26: Ion channels. *British Journal of Pharmacology*, *182*(Suppl 1), S152–S241.

Blin, S., Ben Soussia, I., Kim, E. J., Brau, F., Kang, D., Lesage, F., & Bichet, D. (2016). Mixing and matching TREK/TRAAK subunits generate heterodimeric K_{2P} channels with unique properties. *Proceedings of the National Academy of Sciences of the United States of America*, *113*(15), 4200–4205. https://doi.org/10.1073/pnas.1522748113

Blodgett, D. M., Nowosielska, A., Afik, S., Pechhold, S., Cura, A. J., Kennedy, N. J., Kim, S., Kucukural, A., Davis, R. J., Kent, S. C., Greiner, D. L., Garber, M. G., Harlan, D. M., & Dilorio, P. (2015). Novel observations from next-generation RNA sequencing of highly purified human adult and fetal islet cell subsets. *Diabetes*, *64*(9), 3172–3181.

Chai, S., Wan, X., Ramirez-Navarro, A., Tesar, P. J., Kaufman, E. S., Ficker, E., George, A. L. Jr., & Deschênes, I. (2018). Physiological genomics identifies genetic modifiers of long QT syndrome type 2 severity. *The Journal of Clinical Investigation*, *128*(3), 1043–1056.

Cohen, A., Ben-Abu, Y., Hen, S., & Zilberberg, N. (2008). A novel mechanism for human $K_{2P}2.1$ channel gating. Facilitation of C-type gating by protonation of extracellular histidine residues. *The Journal of Biological Chemistry*, *283*(28), 19448–19455. https://doi.org/10.1074/jbc.M801273200

Curtis, M. J., Alexander, S. P. H., Cortese-Krott, M., Kendall, D. A., Martemyanov, K. A., Mauro, C., Panettieri, R. A. Jr., Papapetropoulos, A., Patel, H. H., Santo, E. E., Schulz, R., Stefanska, B., Stephens, G. J., Teixeira, M. M., Vergnolle, N., Wang, X., & Ferdinandy, P. (2025). Guidance on the planning and reporting of experimental design and analysis. *British Journal of Pharmacology*, *182*, 1413–1415. https://doi.org/10.1111/bph.17441

Danthi, S., Enyeart, J. A., & Enyeart, J. J. (2003). Modulation of native TREK-1 and Kv1.4 K^+ channels by polyunsaturated fatty acids and lysophospholipids. *The Journal of Membrane Biology*, *195*(3), 147–164. https://doi.org/10.1007/s00232-003-0616-0

Decher, N., Kiper, A. K., & Rinné, S. (2017). Stretch-activated potassium currents in the heart: Focus on TREK-1 and arrhythmias. *Progress in Biophysics and Molecular Biology*, *130*(Pt B), 223–232. https://doi.org/10.1016/j.pbiomolbio.2017.05.005

Decher, N., Maier, M., Dittrich, W., Gassenhuber, J., Brüggemann, A., Busch, A. E., & Steinmeyer, K. (2001). Characterization of TASK-4, a novel member of the pH-sensitive, two-pore domain potassium channel family. *FEBS Letters*, *492*(1–2), 84–89. https://doi.org/10.1016/S0014-5793(01)02222-0

Decher, N., Ortiz-Bonnin, B., Friedrich, C., Schewe, M., Kiper, A. K., Rinné, S., Seemann, G., Peyronnet, R., Zumhagen, S., Bustos, D., Kockskämper, J., Kohl, P., Just, S., González, W., Baukrowitz, T., Stallmeyer, B., & Schulze-Bahr, E. (2017). Sodium permeable and "hypersensitive" TREK-1 channels cause ventricular tachycardia. *EMBO Molecular Medicine*, *9*(4), 403–414.

Dobson, J. R., Dadi, P. K., Dickerson, M. T., Nakhe, A. Y., Behera, S., Gibson, S. E., Peachee, S. J., Piron, A., Cnop, M., & Jacobson, D. A.

14765381, 0, Downloaded from https://bpspubs.onlinelibrary.wiley.com/doi/10.1111/bph.70698 by Karlsruher Institut Fur Technologie, Wiley Online Library on [16/11/2026]. See the Terms and Conditions (https://onlinelibrary.wiley.com/terms-and-conditions) on Wiley Online Library for rules of use; OA articles are governed by the applicable Creative Commons License

(2026). The diabetes-associated K^+ channel TALK-2 controls human beta cell endoplasmic reticulum Ca^{2+} handling, which promotes basal insulin release and limits glucose-stimulated insulin secretion. *Diabetologia*, *69*, 1581–1599.

Duprat, F., Girard, C., Jarretou, G., & Lazdunski, M. (2005). Pancreatic two P domain K^+ channels TALK-1 and TALK-2 are activated by nitric oxide and reactive oxygen species. *The Journal of Physiology*, *562*(Pt 1), 235–244. https://doi.org/10.1113/jphysiol.2004.071266

Feliciangeli, S., Chatelain, F. C., Bichet, D., & Lesage, F. (2015). The family of K_{2P} channels: Salient structural and functional properties. *The Journal of Physiology*, *593*(12), 2587–2603. https://doi.org/10.1113/jphysiol.2014.287268

Fink, M., Duprat, F., Lesage, F., Reyes, R., Romey, G., Heurteaux, C., & Lazdunski, M. (1996). Cloning, functional expression and brain localization of a novel unconventional outward rectifier K^+ channel. *The EMBO Journal*, *15*(24), 6854–6862. https://doi.org/10.1002/j.1460-2075.1996.tb01077.x

Friedrich, C., Rinné, S., Zumhagen, S., Kiper, A. K., Silbernagel, N., Netter, M. F., Stallmeyer, B., Schulze-Bahr, E., & Decher, N. (2014). Gain-of-function mutation in TASK-4 channels and severe cardiac conduction disorder. *EMBO Molecular Medicine*, *6*(7), 937–951.

Froese, A., Breher, S. S., Waldeyer, C., Schindler, R. F., Nikolaev, V. O., Rinné, S., Wischmeyer, E., Schlueter, J., Becher, J., Simrick, S., Vauti, F., Kuhtz, J., Meister, P., Kreissl, S., Torlopp, A., Liebig, S. K., Laakmann, S., Müller, T. D., Neumann, J., … Brand, T. (2012). Popeye domain containing proteins are essential for stress-mediated modulation of cardiac pacemaking in mice. *The Journal of Clinical Investigation*, *122*(3), 1119–1130.

Girard, C., Duprat, F., Terrenoire, C., Tinel, N., Fosset, M., Romey, G., Lazdunski, M., & Lesage, F. (2001). Genomic and functional characteristics of novel human pancreatic 2P domain K^+ channels. *Biochemical and Biophysical Research Communications*, *282*(1), 249–256.

Hivelin, C., Béraud-Dufour, S., Devader, C., Abderrahmani, A., Moreno, S., Moha Ou Maati, H., Djillani, A., Heurteaux, C., Borsotto, M., Mazella, J., & Coppola, T. (2016). Potentiation of calcium influx and insulin secretion in pancreatic beta cell by the specific TREK-1 blocker spadin. *Journal of Diabetes Research*, *2016*, 3142175.

Hwang, E. M., Kim, E., Yarishkin, O., Woo, D. H., Han, K. S., Park, N., Bae, Y., Woo, J., Kim, D., Park, M., Lee, C. J., & Park, J. Y. (2014). A disulphide-linked heterodimer of TWIK-1 and TREK-1 mediates passive conductance in astrocytes. *Nature Communications*, *5*, 3227.

Kang, D., Choe, C., & Kim, D. (2005). Thermosensitivity of the two-pore domain K^+ channels TREK-2 and TRAAK. *The Journal of Physiology*, *564*(Pt 1), 103–116. https://doi.org/10.1113/jphysiol.2004.081059

Kang, D., Kim, S. H., Hwang, E. M., Kwon, O. S., Yang, H. Y., Kim, E. S., Choi, T. H., Park, J. Y., Hong, S. G., & Han, J. (2007). Expression of thermosensitive two-pore domain K^+ channels in human keratinocytes cell line HaCaT cells. *Experimental Dermatology*, *16*(12), 1016–1022.

Kennard, L. E., Chumbley, J. R., Ranatunga, K. M., Armstrong, S. J., Veale, E. L., & Mathie, A. (2005). Inhibition of the human two-pore domain potassium channel, TREK-1, by fluoxetine and its metabolite norfluoxetine. *British Journal of Pharmacology*, *144*(6), 821–829. https://doi.org/10.1038/sj.bjp.0706068

Khoubza, L., Chatelain, F. C., Feliciangeli, S., Lesage, F., & Bichet, D. (2021). Physiological roles of heteromerization: Focus on the two-pore domain potassium channels. *The Journal of Physiology*, *599*(4), 1041–1055. https://doi.org/10.1113/JP279870

Khoubza, L., Gilbert, N., Kim, E. J., Chatelain, F. C., Feliciangeli, S., Abelanet, S., Kang, D., Lesage, F., & Bichet, D. (2022). Alkaline-sensitive two-pore domain potassium channels form functional heteromers in pancreatic beta-cells. *The Journal of Biological Chemistry*, *298*(10), 102447.

Kirchmaier, B. C., Poon, K. L., Schwerte, T., Huisken, J., Winkler, C., Jungblut, B., Stainier, D. Y., & Brand, T. (2012). The Popeye domain containing 2 (popdc2) gene in zebrafish is required for heart and skeletal muscle development. *Developmental Biology*, *363*(2), 438–450.

Lengyel, M., Czirjak, G., & Enyedi, P. (2016). Formation of functional heterodimers by TREK-1 and TREK-2 two-pore domain potassium channel subunits. *The Journal of Biological Chemistry*, *291*(26), 13649–13661. https://doi.org/10.1074/jbc.M116.719039

Levitz, J., Royal, P., Comoglio, Y., Wdziekonski, B., Schaub, S., Clemens, D. M., Isacoff, E. Y., & Sandoz, G. (2016). Heterodimerization within the TREK channel subfamily produces a diverse family of highly regulated potassium channels. *Proceedings of the National Academy of Sciences of the United States of America*, *113*(15), 4194–4199.

Lilley, E., Stanford, S. C., Kendall, D. E., Alexander, S. P. H., Cirino, G., Docherty, J. R., George, C. H., Insel, P. A., Izzo, A. A., Ji, Y., Panettieri, R. A., Sobey, C. G., Stefanska, B., Stephens, G., Teixeira, M. M., & Ahluwalia, A. (2020). ARRIVE 2.0 and the British Journal of Pharmacology: Updated guidance for 2020. *British Journal of Pharmacology*, *177*, 3611–3616. https://doi.org/10.1111/bph.15178

Lymperopoulos, A., Altsman, V. L., & Stoicovy, R. A. (2025). Glucagon-like peptide-1 receptor (GLP-1R) signaling: Making the case for a functionally G_s protein-selective GPCR. *International Journal of Molecular Sciences*, *26*(15), 7239. https://doi.org/10.3390/ijms26157239

Maingret, F., Lauritzen, I., Patel, A. J., Heurteaux, C., Reyes, R., Lesage, F., Lazdunski, M., & Honoré, E. (2000). TREK-1 is a heat-activated background K^+ channel. *The EMBO Journal*, *19*(11), 2483–2491.

Maingret, F., Patel, A. J., Lesage, F., Lazdunski, M., & Honore, E. (1999). Mechano- or acid stimulation, two interactive modes of activation of the TREK-1 potassium channel. *The Journal of Biological Chemistry*, *274*(38), 26691–26696. https://doi.org/10.1074/jbc.274.38.26691

Medhurst, A. D., Rennie, G., Chapman, C. G., Meadows, H., Duckworth, M. D., Kelsell, R. E., Gloger, I. I., & Pangalos, M. N. (2001). Distribution analysis of human two pore domain potassium channels in tissues of the central nervous system and periphery. *Brain Research. Molecular Brain Research*, *86*(1–2), 101–114.

Murbartian, J., Lei, Q., Sando, J. J., & Bayliss, D. A. (2005). Sequential phosphorylation mediates receptor- and kinase-induced inhibition of TREK-1 background potassium channels. *The Journal of Biological Chemistry*, *280*(34), 30175–30184. https://doi.org/10.1074/jbc.M503862200

Patel, A. J., Honore, E., Maingret, F., Lesage, F., Fink, M., Duprat, F., & Lazdunski, M. (1998). A mammalian two pore domain mechano-gated S-like K^+ channel. *The EMBO Journal*, *17*(15), 4283–4290. https://doi.org/10.1093/emboj/17.15.4283

Percie du Sert, N., Hurst, V., Ahluwalia, A., Alam, S., Avey, M. T., Baker, M., Browne, W. J., Clark, A., Cuthill, I. C., Dirnagl, U., Emerson, M., Garner, P., Holgate, S. T., Howells, D. W., Karp, N. A., Lazic, S. E., Lidster, K., MacCallum, C. J., Macleod, M., … Würbel, H. (2020). The ARRIVE guidelines 2.0: updated guidelines for reporting animal research. *PLOS Biology*, *18*, e3000410. https://doi.org/10.1371/journal.pbio.3000410

Riel, E. B., Jurs, B. C., Cordeiro, S., Musinszki, M., Schewe, M., & Baukrowitz, T. (2022). The versatile regulation of K_{2P} channels by polyanionic lipids of the phosphoinositide and fatty acid metabolism. *The Journal of General Physiology*, *154*(2), e202112989. https://doi.org/10.1085/jgp.202112989

Rinné, S., Ortiz-Bonnin, B., Stallmeyer, B., Kiper, A. K., Fortmüller, L., Schindler, R. F. R., Herbort-Brand, U., Kabir, N. S., Dittmann, S., Friedrich, C., Zumhagen, S., Gualandi, F., Selvatici, R., Rapezzi, C., Arbustini, E., Ferlini, A., Fabritz, L., Schulze-Bahr, E., Brand, T., & Decher, N. (2020). POPDC2 a novel susceptibility gene for conduction disorders. *Journal of Molecular and Cellular Cardiology*, *145*, 74–83.

Rinné, S., Schick, F., Vowinkel, K., Schütte, S., Krasel, C., Kauferstein, S., Schäfer, M. K., Kiper, A. K., Müller, T., & Decher, N. (2024). Potassium channel TASK-5 forms functional heterodimers with TASK-1 and TASK-3 to break its silence. *Nature Communications*, *15*(1), 7548.

Royal, P., Andres-Bilbe, A., Ávalos Prado, P., Verkest, C., Wdziekonski, B., Schaub, S., Baron, A., Lesage, F., Gasull, X., Levitz, J., & Sandoz, G.

14765381, 0, Downloaded from https://bpspubs.onlinelibrary.wiley.com/doi/10.1111/bph.70698 by Karlsruher Institut Fur Technologie, Wiley Online Library on [16/11/2026]. See the Terms and Conditions (https://onlinelibrary.wiley.com/terms-and-conditions) on Wiley Online Library for rules of use; OA articles are governed by the applicable Creative Commons License

(2019). Migraine-associated TRESK mutations increase neuronal excitability through alternative translation initiation and inhibition of TREK. *Neuron*, *101*(2), 232–245.e6.

Sandoz, G., Douguet, D., Chatelain, F., Lazdunski, M., & Lesage, F. (2009). Extracellular acidification exerts opposite actions on TREK1 and TREK2 potassium channels via a single conserved histidine residue. *Proceedings of the National Academy of Sciences of the United States of America*, *106*(34), 14628–14633. https://doi.org/10.1073/pnas.0906267106

Sandoz, G., Tardy, M. P., Thummler, S., Feliciangeli, S., Lazdunski, M., & Lesage, F. (2008). Mtap2 is a constituent of the protein network that regulates twik-related K^+ channel expression and trafficking. *The Journal of Neuroscience*, *28*(34), 8545–8552. https://doi.org/10.1523/JNEUROSCI.1962-08.2008

Sandoz, G., Thümmler, S., Duprat, F., Feliciangeli, S., Vinh, J., Escoubas, P., Guy, N., Lazdunski, M., & Lesage, F. (2006). AKAP150, a switch to convert mechano-, pH- and arachidonic acid-sensitive TREK K^+ channels into open leak channels. *The EMBO Journal*, *25*(24), 5864–5872.

Schäfer, M. K., Hartwig, N. R., Kalmbach, N., Klietz, M., Anlauf, M., Eiden, L. E., & Weihe, E. (2013). Species-specific vesicular monoamine transporter 2 (VMAT2) expression in mammalian pancreatic beta cells: Implications for optimising radioligand-based human beta cell mass (BCM) imaging in animal models. *Diabetologia*, *56*(5), 1047–1056. https://doi.org/10.1007/s00125-013-2847-7

Schindler, R. F., Scotton, C., Zhang, J., Passarelli, C., Ortiz-Bonnin, B., Simrick, S., Schwerte, T., Poon, K. L., Fang, M., Rinné, S., Froese, A., Nikolaev, V. O., Grunert, C., Müller, T., Tasca, G., Sarathchandra, P., Drago, F., Dallapiccola, B., Rapezzi, C., … Ferlini, A. (2016). POPDC1 (S201F) causes muscular dystrophy and arrhythmia by affecting protein trafficking. *The Journal of Clinical Investigation*, *126*(1), 239–253.

Schmidt, C., Wiedmann, F., Kallenberger, S. M., Ratte, A., Schulte, J. S., Scholz, B., Müller, F. U., Voigt, N., Zafeiriou, M. P., Ehrlich, J. R., Tochtermann, U., Veres, G., Ruhparwar, A., Karck, M., Katus, H. A., & Thomas, D. (2017). Stretch-activated two-pore-domain (K2P) potassium channels in the heart: Focus on atrial fibrillation and heart failure. *Progress in Biophysics and Molecular Biology*, *130*(Pt B), 233–243.

Schmidt, C., Wiedmann, F., Tristram, F., Anand, P., Wenzel, W., Lugenbiel, P., Schweizer, P. A., Katus, H. A., & Thomas, D. (2014). Cardiac expression and atrial fibrillation-associated remodeling of $K_{2P}2.1$ (TREK-1) K^+ channels in a porcine model. *Life Sciences*, *97*(2), 107–115.

Schmidt, C., Wiedmann, F., Voigt, N., Zhou, X. B., Heijman, J., Lang, S., Albert, V., Kallenberger, S., Ruhparwar, A., Szabó, G., Kallenbach, K., Karck, M., Borggrefe, M., Biliczki, P., Ehrlich, J. R., Baczkó, I., Lugenbiel, P., Schweizer, P. A., Donner, B. C., … Thomas, D. (2015). Upregulation of $K_{2P}3.1$ K^+ current causes action potential shortening in patients with chronic atrial fibrillation. *Circulation*, *132*(2), 82–92.

Schmidt, C., Wiedmann, F., Zhou, X. B., Heijman, J., Voigt, N., Ratte, A., Lang, S., Kallenberger, S. M., Campana, C., Weymann, A., De Simone, R., Szabo, G., Ruhparwar, A., Kallenbach, K., Karck, M., Ehrlich, J. R., Baczkó, I., Borggrefe, M., Ravens, U., … Thomas, D. (2017). Inverse remodelling of $K_{2P}3.1$ K^+ channel expression and action potential duration in left ventricular dysfunction and atrial fibrillation: Implications for patient-specific antiarrhythmic drug therapy. *European Heart Journal*, *38*(22), 1764–1774.

Simrick, S., Schindler, R. F., Poon, K. L., & Brand, T. (2013). Popeye domain-containing proteins and stress-mediated modulation of cardiac pacemaking. *Trends in Cardiovascular Medicine*, *23*(7), 257–263. https://doi.org/10.1016/j.tcm.2013.02.002

Staudacher, I., Illg, C., Chai, S., Deschenes, I., Seehausen, S., Gramlich, D., Müller, M. E., Wieder, T., Rahm, A. K., Mayer, C., Schweizer, P. A., Katus, H. A., & Thomas, D. (2018). Cardiovascular pharmacology of $K_{2P}17.1$ (TASK-4, TALK-2) two-pore-domain K^+ channels. *Naunyn-Schmiedeberg's Archives of Pharmacology*, *391*(10), 1119–1131.

Suzuki, Y., Tsutsumi, K., Miyamoto, T., Yamamura, H., & Imaizumi, Y. (2017). Heterodimerization of two pore domain K^+ channel TASK1 and TALK2 in living heterologous expression systems. *PLoS ONE*, *12*(10), e0186252. https://doi.org/10.1371/journal.pone.0186252

Talley, E. M., Solorzano, G., Lei, Q., Kim, D., & Bayliss, D. A. (2001). Cns distribution of members of the two-pore-domain (*KCNK*) potassium channel family. *The Journal of Neuroscience*, *21*(19), 7491–7505. https://doi.org/10.1523/JNEUROSCI.21-19-07491.2001

Tertyshnikova, S., Knox, R. J., Plym, M. J., Thalody, G., Griffin, C., Neelands, T., Harden, D. G., Signor, L., Weaver, D., Myers, R. A., & Lodge, N. J. (2005). BL-1249 [(5,6,7,8-tetrahydro-naphthalen-1-yl)-[2-(1H-tetrazol-5-yl)-phenyl]-amine]: A putative potassium channel opener with bladder-relaxant properties. *The Journal of Pharmacology and Experimental Therapeutics*, *313*(1), 250–259.

Unudurthi, S. D., Wu, X., Qian, L., Amari, F., Onal, B., Li, N., Makara, M. A., Smith, S. A., Snyder, J., Fedorov, V. V., Coppola, V., Anderson, M. E., Mohler, P. J., & Hund, T. J. (2016). Two-pore K^+ channel TREK-1 regulates sinoatrial node membrane excitability. *Journal of the American Heart Association*, *5*(4), e002865.

Varshney, A., Scott, L. J., Welch, R. P., Erdos, M. R., Chines, P. S., Narisu, N., Albanus, R. D., Orchard, P., Wolford, B. N., Kursawe, R., Vadlamudi, S., Cannon, M. E., Didion, J. P., Hensley, J., Kirilusha, A., NISC Comparative Sequencing Program, Bonnycastle, L. L., Taylor, D. L., Watanabe, R., … Stitzel, M. L. (2017). Genetic regulatory signatures underlying islet gene expression and type 2 diabetes. *Proceedings of the National Academy of Sciences of the United States of America*, *114*(9), 2301–2306.

Viatchenko-Karpinski, V., Ling, J., & Gu, J. G. (2018). Characterization of temperature-sensitive leak K^+ currents and expression of TRAAK, TREK-1, and TREK2 channels in dorsal root ganglion neurons of rats. *Molecular Brain*, *11*(1), 40. https://doi.org/10.1186/s13041-018-0384-5

Vissing, J., Johnson, K., Töpf, A., Nafissi, S., Díaz-Manera, J., French, V. M., Schindler, R. F., Sarathchandra, P., Løkken, N., Rinné, S., Freund, M., Decher, N., Müller, T., Duno, M., Krag, T., Brand, T., & Straub, V. (2019). *POPDC3* gene variants associate with a new form of limb girdle muscular dystrophy. *Annals of Neurology*, *86*(6), 832–843.

Weber, W. (1999). Ion currents of *Xenopus laevis* oocytes: State of the art. *Biochimica et Biophysica Acta*, *1421*(2), 213–233. https://doi.org/10.1016/s0005-2736(99)00135-2

Wiedmann, F., Frey, N., & Schmidt, C. (2021). Two-pore-domain potassium (K_{2P}) channels: Cardiac expression patterns and disease-specific remodelling processes. *Cells*, *10*(11), 2914. https://doi.org/10.3390/cells10112914

Zhu, R., Pan, X., Wang, S., Qiu, Z., Gu, C., Yao, X., & Li, W. (2023). Updated skin transcriptomic atlas depicted by reciprocal contribution of single-nucleus RNA sequencing and single-cell RNA sequencing. *Journal of Dermatological Science*, *111*(2), 22–31. https://doi.org/10.1016/j.jdermsci.2023.06.005

SUPPORTING INFORMATION

Additional supporting information can be found online in the Supporting Information section at the end of this article.

How to cite this article: Schütte, S., Schick, F., De Martino, E., Schmitz, H., Zander, K. E. S., Holz, F., Sauer, P., Mildeberger, L., Linder, M., Loewe, A., Kiper, A. K., Kauferstein, S., Schäfer, M. K.-H., Rinné, S., & Decher, N. (2026). Crossing subfamily borders: Mechanosensitive TREK-1 and alkaline-activated TASK-4 form heterodimers with unique functional and pharmacological properties. *British Journal of Pharmacology*, 1–15. https://doi.org/10.1111/bph.70698

14765381, 0, Downloaded from https://bpspubs.onlinelibrary.wiley.com/doi/10.1111/bph.70698 by Karlsruher Institut Fur Technologie, Wiley Online Library on [16/11/2026]. See the Terms and Conditions (https://onlinelibrary.wiley.com/terms-and-conditions) on Wiley Online Library for rules of use; OA articles are governed by the applicable Creative Commons License